

Wilfrid Laurier University

Scholars Commons @ Laurier

---

Theses and Dissertations (Comprehensive)

---

1994

## A test of the multiquadric technique of interpolation with an application to fluid speeds in a river (Ontario)

James Patrick Dozois  
*Wilfrid Laurier University*

Follow this and additional works at: <https://scholars.wlu.ca/etd>



Part of the [Geographic Information Sciences Commons](#)

---

### Recommended Citation

Dozois, James Patrick, "A test of the multiquadric technique of interpolation with an application to fluid speeds in a river (Ontario)" (1994). *Theses and Dissertations (Comprehensive)*. 326.  
<https://scholars.wlu.ca/etd/326>

This Thesis is brought to you for free and open access by Scholars Commons @ Laurier. It has been accepted for inclusion in Theses and Dissertations (Comprehensive) by an authorized administrator of Scholars Commons @ Laurier. For more information, please contact [scholarscommons@wlu.ca](mailto:scholarscommons@wlu.ca).



National Library  
of Canada

Acquisitions and  
Bibliographic Services Branch

395 Wellington Street  
Ottawa Ontario  
K1A 0N4

Bibliothèque nationale  
du Canada

Direction des acquisitions et  
des services bibliographiques

395 rue Wellington  
Ottawa (Ontario)  
K1A 0N4

*Notice - Avis*

*Notice - Avis*

## NOTICE

The quality of this microform is heavily dependent upon the quality of the original thesis submitted for microfilming. Every effort has been made to ensure the highest quality of reproduction possible.

If pages are missing, contact the university which granted the degree.

Some pages may have indistinct print especially if the original pages were typed with a poor typewriter ribbon or if the university sent us an inferior photocopy.

Reproduction in full or in part of this microform is governed by the Canadian Copyright Act, R.S.C. 1970, c. C-30, and subsequent amendments.

## AVIS

La qualité de cette microforme dépend grandement de la qualité de la thèse soumise au microfilmage. Nous avons tout fait pour assurer une qualité supérieure de reproduction.

S'il manque des pages, veuillez communiquer avec l'université qui a conféré le grade.

La qualité d'impression de certaines pages peut laisser à désirer, surtout si les pages originales ont été dactylographiées à l'aide d'un ruban usé ou si l'université nous a fait parvenir une photocopie de qualité inférieure.

La reproduction, même partielle, de cette microforme est soumise à la Loi canadienne sur le droit d'auteur, SRC 1970, c. C-30, et ses amendements subséquents.

**Canada**

A TEST OF THE MULTIQUADRIC TECHNIQUE  
OF INTERPOLATION  
WITH AN APPLICATION TO FLUID SPEEDS  
IN A RIVER

BY

JAMES P. DOZOIS

B.A., Wilfrid Laurier University, 1991

THESIS

Submitted to the Department of Geography  
in partial fulfilment of the requirements  
for the Masters of Arts degree  
Wilfrid Laurier University  
1994

©James P. Dozois 1994



National Library  
of Canada

Bibliothèque nationale  
du Canada

Acquisitions and  
Bibliographic Services Branch

Direction des acquisitions et  
des services bibliographiques

395 Wellington Street  
Ottawa, Ontario  
K1A 0N4

395, rue Wellington  
Ottawa (Ontario)  
K1A 0N4

*Your file / Votre référence*

*Our file / Notre référence*

THE AUTHOR HAS GRANTED AN  
IRREVOCABLE NON-EXCLUSIVE  
LICENCE ALLOWING THE NATIONAL  
LIBRARY OF CANADA TO  
REPRODUCE, LOAN, DISTRIBUTE OR  
SELL COPIES OF HIS/HER THESIS BY  
ANY MEANS AND IN ANY FORM OR  
FORMAT, MAKING THIS THESIS  
AVAILABLE TO INTERESTED  
PERSONS.

L'AUTEUR A ACCORDE UNE LICENCE  
IRREVOCABLE ET NON EXCLUSIVE  
PERMETTANT A LA BIBLIOTHEQUE  
NATIONALE DU CANADA DE  
REPRODUIRE, PRETER, DISTRIBUER  
OU VENDRE DES COPIES DE SA  
THESE DE QUELQUE MANIERE ET  
SOUS QUELQUE FORME QUE CE SOIT  
POUR METTRE DES EXEMPLAIRES DE  
CETTE THESE A LA DISPOSITION DES  
PERSONNE INTERESSEES.

THE AUTHOR RETAINS OWNERSHIP  
OF THE COPYRIGHT IN HIS/HER  
THESIS. NEITHER THE THESIS NOR  
SUBSTANTIAL EXTRACTS FROM IT  
MAY BE PRINTED OR OTHERWISE  
REPRODUCED WITHOUT HIS/HER  
PERMISSION.

L'AUTEUR CONSERVE LA PROPRIETE  
DU DROIT D'AUTEUR QUI PROTEGE  
SA THESE. NI LA THESE NI DES  
EXTRAITS SUBSTANTIELS DE CELLE-  
CI NE DOIVENT ETRE IMPRIMES OU  
AUTREMENT REPRODUITS SANS SON  
AUTORISATION.

ISBN 0-612-01813-X

Canada

## **ABSTRACT**

Hardy's (1971) technique of interpolation was tested using fluid speed data from Big Otter Creek, a gravel bed stream, in South-Western Ontario. Fourteen cross-sections were selected from a 500 m-long reach of the river. Each cross-section was divided into 10 verticals. Fluid speed was sampled at different positions in these verticals starting at 0.025 m off the channel bed using an electromagnetic current metre. Bed roughness at each cross-section was determined by collecting samples of the bed material and by measuring the long, intermediate and short axes of particles at the 10 verticals.

To test the multiquadric technique of interpolation, known fluid speeds from the collected data sets were systematically and randomly removed from the cross-section and plan views. These new, smaller data sets were then used as input for a series of computer programs which generated a multiquadric surface. The interpolated fluid speeds were compared against the known fluid speeds to determine the magnitude of the errors.

The results show that the largest error values occurred in the near bed region and in areas with steep velocity gradients. Of the two types of analyses, cross-section and plan view, the plan view had the largest errors. No difference in error magnitude or location was identified between the random and systematic analyses.

## **ACKNOWLEDGEMENTS**

I would like to thank my Examining Committee - Dr. Moore, chairperson; Drs. Hall and Kott, external readers; and Drs. Saunderson and Byrne, advisors. Dr. Saunderson, the thesis primary advisor, deserves special thanks for all the advice and support that he gave me. Dr. Byrne's comments throughout the thesis were also very helpful and appreciated. Thank You both very much.

This thesis would not have been possible without the invaluable field assistance which I received from a number people. John Beebe's field help and advice have made this thesis better. Rich Pyrcce and Dave Crooks were also great field assistants.

I would also like to thank all my friends who provided support and encouragement throughout my years at Laurier.

Finally, I would like to thank my parents and brothers, Mark and Rob whose support throughout my education will never be forgotten. Thank You All.

.

**TABLE OF CONTENTS**

ABSTRACT . . . . . i

ACKNOWLEDGEMENTS . . . . . ii

TABLE OF CONTENTS . . . . . iii

LIST OF FIGURES . . . . . v

LIST OF TABLES . . . . . vi

CHAPTER 1: INTRODUCTION AND BACKGROUND INFORMATION . . . . . 1

    1.1 INTRODUCTION . . . . . 1

    1.2 BACKGROUND INFORMATION . . . . . 3

    1.3 APPLICATIONS TO FLUID SPEEDS IN A RIVER . . . . . 12

    1.4 GOAL AND OBJECTIVES . . . . . 14

CHAPTER 2: STUDY AREA AND FIELD METHODOLOGY . . . . . 16

    2.1 STUDY AREA . . . . . 16

    2.2 COLLECTION OF FIELD DATA . . . . . 19

    2.3 PARTICLE SIZE AND DISCUSSION . . . . . 23

    2.4 INTERPRETATION OF SEDIMENT CURVES . . . . . 28

    2.5 MEASURED PARTICLE RESULTS . . . . . 30

    2.6 SUSPENDED SEDIMENT AND TEMPERATURE . . . . . 33

    2.7 BED LOAD SAMPLING . . . . . 34

CHAPTER 3: TESTING THE MULTIQUADRIC TECHNIQUE . . . . . 35

    3.1 INTRODUCTION . . . . . 35

    3.2 COMPUTER PROGRAMS . . . . . 36

    3.3 TESTING THE METHODOLOGY . . . . . 40

        3.3.1 INTRODUCTION . . . . . 40

    3.4 TESTING PROCEDURE . . . . . 42

        3.4.1 CONVERSION OF FIELD DATA (CROSS-SECTION ANALYSES ONLY) . . . . . 42

        3.4.2 GENERATION OF PLAN VIEW GRID . . . . . 42

        3.4.3 SELECTION OF CONTROL POINTS . . . . . 43

            3.4.3.1 SYSTEMATIC REMOVAL OF POINTS - CROSS-SECTION . . . . . 43

            3.4.3.2 SYSTEMATIC REMOVAL OF POINTS - PLAN VIEW . . . . . 45

            3.4.3.3 RANDOM REMOVAL OF POINTS . . . . . 45

        3.4.4 EXECUTION OF PROGRAMS . . . . . 47

        3.4.5 CALCULATION AND GRAPHING OF ERRORS . . . . . 51

CHAPTER 4: RESULTS . . . . . 53

    4.1 SYSTEMATIC REMOVAL OF POINTS: CROSS-SECTION ANALYSES . . . . . 53

    4.2 RESULTS: RANDOM REMOVAL OF POINTS . . . . . 61

    4.3 ANALYSIS AND INTERPRETATION . . . . . 68

        4.3.1 INTRODUCTION . . . . . 68

        4.3.2 GEOGRAPHIC DISTRIBUTION OF ERROR -

CROSS-SECTION ANALYSES . . . . .	69
4.3.3 DISTRIBUTION OF ERROR AND NEAREST NEIGHBOUR POINTS . . . . .	71
4.3.4 MAGNITUDE OF ERROR - CROSS-SECTION AND PANEL RUNS COMPARED . . . . .	74
4.3.5 GEOGRAPHIC DISTRIBUTION OF ERRORS - PANEL RUNS . . . . .	76
4.3.6 RELATIVE ERROR AND POSITION IN THE CROSS-SECTION . . . . .	76
4.3.7 MULTIQUADRICS AND VELOCITY PROFILES . . . . .	78
. . . . .	84
4.4 DISTRIBUTION OF ERROR - PLAN VIEW - SVR . . . . .	85
4.4.1 RELATIVE ERROR . . . . .	85
4.4.1.1 BED SPEEDS . . . . .	85
4.4.1.2 SURFACE SPEEDS . . . . .	86
4.4.1.3 AVERAGE SPEEDS . . . . .	86
4.4.2.1 BED SPEEDS . . . . .	87
4.4.2.3 AVERAGE SPEEDS . . . . .	88
4.4.3 DISCUSSION . . . . .	90
4.5 DISTRIBUTION OF ERROR - PLAN VIEW - PANEL RUNS . . . . .	91
4.5.1 RELATIVE ERROR . . . . .	91
4.5.1.1 BED SPEEDS . . . . .	91
4.5.1.2 SURFACE SPEEDS . . . . .	92
4.5.1.3 AVERAGE SPEEDS . . . . .	93
4.5.2 ABSOLUTE ERROR . . . . .	95
4.5.2.1 BED SPEEDS . . . . .	95
4.5.2.2 SURFACE SPEEDS . . . . .	95
4.5.2.3 AVERAGE VALUES . . . . .	96
4.5.3 DISCUSSION . . . . .	96
CHAPTER 5: DISCUSSION . . . . .	98
5.1 VELOCITY PROFILES AND MULTIQUADRICS . . . . .	98
5.2 COMPARISON OF CROSS-SECTION AND PLAN VIEW ANALYSES . . . . .	102
5.3 SAMPLING PROCEDURES . . . . .	104
5.4 BED ROUGHNESS AND TURBULENCE AND MULTIQUADRICS . . . . .	105
CHAPTER 6 CONCLUSIONS . . . . .	111
6.1 SUMMARY . . . . .	111
6.2 FUTURE RESEARCH . . . . .	117
REFERENCES . . . . .	119



## LIST OF FIGURES

FIGURE 2.1A LOCATION OF STUDY SITE . . . . .	17
FIGURE 2.1B STUDY AREA . . . . .	18
Figure 2.2 SCHEMATIC OF TRANSIT DIVISION FOR A CROSS-SECTION LOCATED IN THE MEANDER . . . . .	20
FIGURE 2.3A PARTICLE SIZE ANALYSIS CROSS-SECTION 2 PANELS 1-5 . . . . .	25
FIGURE 2.3B PARTICLE SIZE ANALYSIS CROSS-SECTION 2 PANELS 6-10 . . . . .	26
FIGURE 2.4 PARTICLE SIZE ANALYSIS CROSS-SECTIONS 8-11	27
FIGURE 2.5 PARTICLE SIZE ANALYSIS CROSS-SECTIONS 12-14	28
FIGURE 2.6 DISTRIBUTION OF PARTICLE SIZE (MEASURED B AXIS) . . . . .	30
FIGURE 2.7 AVERAGE MEASURED PARTICLE SIZE CROSS-SECTIONS 1 TO 5 . . . . .	31
FIGURE 2.8 AVERAGE MEASURED PARTICLE SIZE CROSS-SECTIONS 6 TO 11 . . . . .	31
FIGURE 2.9 AVERAGE MEASURED PARTICLE SIZE CROSS-SECTIONS 12 TO 14 . . . . .	31
FIGURE 4.1A ABSOLUTE ERROR - CS 8 . . . . .	62
FIGURE 4.1B RELATIVE ERROR - CS 8 . . . . .	62
FIGURE 4.2A ABSOLUTE ERROR - CS 9 . . . . .	63
FIGURE 4.2B RELATIVE ERROR - CS 9 . . . . .	63
FIGURE 4.3A ABSOLUTE ERROR - CS 10 . . . . .	64
FIGURE 4.3B RELATIVE ERROR - CS 10 . . . . .	64
FIGURE 4.4A ABSOLUTE ERROR - CS 11 . . . . .	65
FIGURE 4.4B RELATIVE ERROR - CS 11 . . . . .	65
FIGURE 4.5 AVERAGE NEAREST NEIGHBOUR VS. INTERPOLATED VALUES . . . . .	73
FIGURE 4.6 RELATIVE ERROR AS A FUNCTION OF LOCATION IN PROFILE CROSS-SECTION 9 . . . . .	77
FIGURE 4.7 VELOCITY PROFILES - PANEL 5, CROSS-SECTION 8 . . . . .	80
FIGURE 4.8 VELOCITY PROFILES FOR PANEL 6, CROSS-SECTION 8, PANEL REMOVAL . . . . .	82
FIGURE 4.9 VELOCITY PROFILES FOR PANEL 5, CROSS-SECTION 8, R813 . . . . .	83
FIGURE 4.10A AND B - ERROR DISTRIBUTION - PLAN VIEW - SVR	
FIGURE 4.10A RELATIVE ERROR 4.10B ABSOLUTE ERROR . . .	89
FIGURES 4.11A AND B - ERROR DISTRIBUTION - PLAN VIEW - PANEL RUNS	
FIGURE 4.11A RELATIVE ERROR FIGURE 11B ABSOLUTE ERROR	94
FIGURE 5.1 MULTIQUADRICS AND CURVE FITTING: PANEL 4, CROSS-SECTION 8 . . . . .	102
FIGURE 5.2 RELATIVE ROUGHNESS AND AVERAGE RELATIVE ERROR . . . . .	108

## LIST OF TABLES

TABLE 1.0 APPLICATIONS OF THE MULTIQUADRIC TECHNIQUE . . . . .	8
TABLE 2.1 SITE SUMMARY . . . . .	22
TABLE 2.2 GRAPHIC MEAN (PHI UNITS $\Phi$ ) . . . . .	24
TABLE 2.3 SUSPENDED SEDIMENT CONCENTRATIONS AND TEMPERATURE . . . . .	33
TABLE 3.1 XY.DAT . . . . .	38
TABLE 3.2 Z.DAT . . . . .	38
TABLE 3.3 OUTPUT FROM MATRX1.DAT . . . . .	39
TABLE 3.4 CVEC OUTPUT . . . . .	39
TABLE 3.5 SUMMARY OF SYSTEMATIC REMOVAL OF POINTS - CROSS-SECTION ANALYSES . . . . .	44
TABLE 3.6 SUMMARY OF SYSTEMATIC REMOVAL OF POINTS - PLAN VIEW . . . . .	45
TABLE 3.7A AWK COMMANDS USED TO LOCATE POINTS . . . . .	49
TABLE 3.7B AWK COMMANDS USED TO BREAK DATA INTO BLOCKS	50
TABLE 4.1 SUMMARY OF ABSOLUTE AND RELATIVE ERRORS - CROSS-SECTION 11 . . . . .	54
TABLE 4.2 SUMMARY OF ABSOLUTE AND RELATIVE ERROR - PANEL REMOVAL RUNS - CROSS-SECTION 11 . . . . .	56
TABLE 4.3 DIFFERENCES IN INTERPOLATED VALUES . . . . .	58
TABLE 4.4 LOCATION AND ANALYSES WITH ERROR VALUES OF 0	58
TABLE 4.5 SUMMARY OF ABSOLUTE AND RELATIVE ERRORS - CROSS-SECTION 8 . . . . .	59
TABLE 4.6 SUMMARY OF ABSOLUTE AND RELATIVE ERRORS - CROSS-SECTION 9 . . . . .	59
TABLE 4.7 SUMMARY OF ABSOLUTE AND RELATIVE ERRORS - CROSS SECTION 10 . . . . .	60
TABLE 4.8 SUMMARY OF ABSOLUTE AND RELATIVE ERRORS - CROSS-SECTION 11 . . . . .	60
TABLE 4.9 INTERPOLATED VALUES FOR PANEL 7 - RANDOM ANALYSES . . . . .	67
TABLE 4.10 RESULTS OF NO-SLIP CONDITION TEST: CROSS- SECTION 10 . . . . .	84

## **CHAPTER 1: INTRODUCTION AND BACKGROUND INFORMATION**

### **1.1 INTRODUCTION**

In the analysis of fluid flows in a river, two terms are used - velocity and speed. Velocity has both a magnitude and a direction, while speed has just a magnitude. In this thesis, only fluid speed is used and analyzed, but both terms, speed and velocity will be used in reference to magnitude of the fluid flow. The only directional component of flow was either positive, if the flow was moving downstream, or negative, if there was reverse flow. While it would have been desirable to measure the velocity, that is the vectorial component and magnitude of flow, the Marsh-McBirney 512 directional electromagnetic current metre was not operational at the time of sampling.

Fluid speed pattern analysis is an important component in the study of rivers and river processes. Examination of fluid speeds is needed for the calculation of many variables used in fluvial geomorphology, for example shear stress, Reynolds number and Froude numbers. Variations in speed can create areas of aggradation and deposition along and across reaches of a river (eg. Menard, 1950; Sundborg, 1967; Vanoni, 1966; Meland and Norrman, 1966; Baker and Ritter, 1975; Komar, 1987). The formation of in-channel features, such as point bars and transverse ridges, has been related to changes in speed (eg. Martini, 1977; Bridge and Gabel, 1992; Best, 1988).

Also, speed variations can have direct and indirect impacts on ecosystems. Example of direct influences include removal of spawning areas and silting over of spawning areas speed, while an indirect result would be the influence of speed on pollution dispersal.

In order to examine fluid speeds effectively for these various applications, speeds must be sampled at different locations, both across a river channel and along a stream's length (ie. in plan view). Unfortunately, it is not always feasible to accurately sample rivers in sufficient detail to examine variations in speed. Limitations to sampling include lack of equipment, time, financial and personnel constraints. Often the most significant hydrological events, such as rapid changes in stage, cannot be safely surveyed, yet are very important in the study of channel morphology (Dietrich and Gallinatti, 1991). To examine these high stage events, researchers have sampled from secure platforms (e.g. bridges), have limited their collection to times of safe sampling or have relied on values based on rating curves or other derived data (e.g. discharge calculated from flood deposits). A way to examine fluid speed patterns based on a limited number of sampled points is needed to examine changes to channel morphology.

Interpolation, a method by which a larger data set is created based on a given number of points, has been used in the creation of surfaces, such as elevations on a topographic

map sheet. The production of a contour map is based on the interpolation of elevations from known, measured points. Similarly, other surfaces can be created using interpolation - examples include precipitation, ocean temperatures and fluid speeds.

In order to generate a useful fluid speed surface, a method by which speeds can be sampled and interpolated is needed. This surface can then be studied and inferences about potential areas of erosion and deposition and areas of preferential habitat made.

## **1.2 BACKGROUND INFORMATION**

Estimation of a point can involve two processes, interpolation and extrapolation. Watson (1992, p. 102) defined interpolation as "... an operation on multivariate data, so it has a natural spatial domain, the convex hull of the data set. The convex hull is the region enclosed by a connecting set of straightline segments around the perimeter....". If a point is determined outside of this convex hull, the process is extrapolation (Watson, 1992, p. 102). Although points may lie outside this convex hull, some interpolating procedures may still provide "remarkable surficial features" in this outside region (Watson, personal communication).

Interpolation techniques can be classified into two categories: global and local. A global technique of

interpolation is one where "the interpolant is dependent on all data points, and addition or deletion of a data point, or a change in one of the coordinates of a data point will propagate throughout the domain of definition" (Franke, 1982, p. 182). In other words, all points in the sampled space will have an influence on the interpolant. Local interpolation routines are those in which only the near-by data points are used to determine an interpolant (Schiro and Williams, 1984). A problem with local interpolation routines is the determination of nearest neighbours (ie. nearest data points) - at what distance does the influence of neighbouring points become negligible in the interpolation (Franke, 1982)?

Hardy's multiquadric technique of interpolation is a global technique that passes through all the original, or control points (Hardy, 1971, 1990; Franke, 1982). The general form of the multiquadric surface (Hardy, 1971; Hardy and Goofert, 1975; Sirayanone, 1988) is:

$$(1) \quad \sum_{i=1}^n c_i [q(x_i, y_i, x, y)] = z$$

where,  $z$  is a function of  $x$  and  $y$  which results from the summation of a single class of quadric surfaces and  $x_i$  and  $y_i$  are the coordinates of the apex of the cone (Hardy, 1971).

There are a number of different quadric surfaces:

(2) Hyperbolic Quadric:

$$Q = C_3[(X-X_1)^2 + (Y-Y_1)^2 + C^2]^{-1/2}$$

(3) Reciprocal Hyperbolic Quadric:

$$Q = C_3[(X-X_1)^2 + (Y-Y_1)^2 + C^2]^{-1/2}$$

(4) Conic Quadric:

$$Q = C_3[(X-X_1)^2 + (Y-Y_1)^2 + C^2]^{-1/2}, \text{ where } C=0$$

(5) Parabolic Quadric:

$$Q = C_3[(X-X_1)^2 + (Y-Y_1)^2 + C^2]^{-1/2}, \text{ where } C = 0$$

(modified from Hardy, 1971, 1990; Schiro and Williams, 1984. In equations 4 and 5, the constant, C, is equal to 0. The term does not need to be in the equations, in fact most uses of the conic and parabolic surface do not list the term, but it has been included here for the purpose of consistency.

The most widely used quadric surface is the cone, (Saunderson, 1992). The value selected for C will influence the shape of the surface generated (Sirayanone, 1988). Depending on the application, the conic surface may not be the most ideal surface. In the original paper, Hardy (1971) used the cone model (Eq. 4) to generate topographical surfaces. He created fictitious models of topography from which he sampled control points to use as input for the multiquadric system of equations and against which comparisons would be made with the multiquadric surface.

In the first experiment Hardy (1971) selected 13 significant data points. These 13 significant data points

were related to the boundary of the mapped area, to highs and lows in the region as well as to a number of interior points to further represent the area. Using these 13 points, the multiquadric surface visually represented the area fairly accurately, however, a drainage area in the lower corner of the map was not very well represented. Hardy explained this deficiency as the result of the low sampled point density in the drainage area (Hardy, 1971).

For a second experiment the number of control points was increased from 13 to 38, thereby increasing the point density. The result was a map that was a better visual fit to the original than the map based on the 13 points; however, this increased number of points created a saddle in an area that did not exist in the fictitious model. This deficiency did not seem to alter the visual accuracy of the map, however (Hardy, 1971).

Hardy ran another experiment to determine the accuracy of joint map edges by creating another fictitious model. This second model, an extension of the first model used in the experiments above used 34 significant points, including 5 that were common to the other map. However, the selection of the control points in this experiment was done in a less careful manner than in the other experiments (see above). The result was a good fit between the common boundary area. Hardy calculated the discrepancies between the multiquadric model and the fictitious model and found that the mean discrepancy



was one-tenth of the contour interval and the maximum was one-third of the contour interval (1971, p. 1912).

Next, Hardy joined the two fictitious models to form one map sheet and selected 72 significant points - 38 from the first set of experiments and 34 from the second set. The contour map produced from these 72 points was visually similar to the original model.

A third fictitious contour model was created and 41 points were randomly selected along regularly spaced profiles. "The resemblance of the multiquadric surface to the contour model shows that using such a random scanning mode works reasonably well for an uncomplicated subsurface case (1971, p. 1913). The contours based on the multiquadric data were extrapolated past the sampled regions with results that appeared to be logical.

As a further test of the method Hardy used the data from an earlier study that used polynomials and Fourier analysis to represent topography based data sampled off a USGS map. Hardy concluded that although the multiquadric surface was deficient in its representation of the size and shapes of the hills, the reason was probably poor point selection (Hardy, 1971, p. 1914).

In addition to Hardy's (1971) topographical study, numerous applications employing the multiquadric technique have been developed. Hardy (1990) identified the following as areas to which multiquadrics have been applied: geodesy,

surveying and mapping, geophysics, photogrammetry and remote sensing, digital terrain modelling and hydrology. Table 1 summarizes some of these studies/applications.

**TABLE 1.0 APPLICATIONS OF THE MULTIQUADRIC TECHNIQUE**

Application	Reference(s)
Air Temperature	Sirayanone, 1988
Wind Speed	Sirayanone, 1988
Rainfall	Shaw and Lynn, 1972 Lee, Lynn and Shaw, 1974 Tabios and Salas, 1985
Photogrammetry	Hardy, 1977
Topography	Hardy, 1971 Hardy, 1972 Schiro and Williams, 1984
Mining	Sirayanone, 1988
Geodesy	Hadgiieorge and Trotter, 1977 Hardy and Gopfert, 1975
Fluid Speeds	Saunderson 1992 Hassan et al., 1992 Saunderson, 1994 Saunderson and Brooks (in press)

Shaw and Lynn (1972) used the multiquadric technique to

interpolate areal rainfall. As part of their study, multiquadrics were compared to bi-cubic splines using a theoretical data set for rainfall sampled on a grid. The cone model (Eq. 4) with  $C=0$  was used. The bi-cubic splines performed a little better statistically, but the multiquadric method was within 0.3 % of areal average rainfall. Based on this result, the authors concluded that multiquadrics could be used for gridded data. Hardy (1990) in a review of this use of the method, commented that only the cone model was used and that perhaps the optimum value of  $C$  was not selected. If a different value was used, he suggested that perhaps the statistical agreement would have been better or perfect.

Real rainfall data is seldom collected from a grid system; the locations of raingauges is more random. Because of this, Shaw and Lee (1972) compared multiquadrics against standard hydrological techniques for the interpolation of areal rainfall - Thiessen polygons, arithmetic mean and the isohyetal method. They concluded that for real areal rainfall sampled from an irregular network of gauges the accuracy of the multiquadric procedure was comparable to the standard techniques, but that it had the advantage of being faster and less subjective (1972, p. 432).

In a later study using the same areal rainfall data set Lee, Lynn and Shaw (1974) used two quadric surfaces - the cone and the hyperboloids (Eqs. 4 and 2). They concluded that the hyperboloid gave a smoother surface and because of this may be

better to use for areal rainfall. The results between the two methods were similar for simple storm data, but the cone was preferred because of its simplicity, efficiency and objectiveness of the procedure (1974, p. 317). Determining the value of C in the hyperboloid is a subjective process.

Tabios and Salas (1985) compared a number of interpolation routines for rainfall data, including kriging, optimal interpolation, multiquadrics (using the cone model) and Thiessen polygons. To test the various routines, known points in a data set were suppressed and the interpolated values were then compared against the real values. Their study found that kriging and optimal interpolation gave the best results, but that the multiquadric method "is almost as good as the other two" (1985, p. 365).

Sirayanone (1988) compared the multiquadrics technique against kriging for a number of applications - air temperature, wind velocities (vectorial data), mining and pollution modelling. The mining and pollution modelling involved 3 dimensions. The multiquadric technique had a lower root mean square error than kriging. Also, because kriging required extensive preprocessing, the multiquadric technique was more efficient in terms of time and computer space.

In his thesis, Sirayanone (1988) reviewed and discussed a study by Brooks (1971, as cited in Sirayanone (1988)), in which 8 geomorphologically diverse areas were selected as tests for the multiquadric equations of topography (the data

was selected from USGS topographic maps). Two types of tests were performed: data sampled at significant points and data sampled from a grid pattern. The multiquadric technique represented the test surfaces very well. The accuracy of the surface could be increased by increasing the number of points in significant areas, such as ridges and saddles. The cone model ( $C=0$ ) and hyperboloids ( $C\neq 0$ ) were tested. For the hyperboloids, the value of the constant ranged from 0.001 to 0.0001. It was concluded that the cone model was better for the tops of hills and that the hyperboloid was better for lower elevations and gently sloping hills (Sirayanone, 1988).

Schiro and Williams (1984) used multiquadrics for hydrographic data (sea floor contours). The data used were irregularly sampled elevations along parallel tracks. Pickerall (1979, as cited in Schiro and Williams 1984) tested different multiquadric surfaces using similar data and concluded that the cone model was the best. They also referred to the results of Franke (1979, as cited in Schiro and Williams 1984) and Hein (1979, as cited in Schiro and Williams 1984) who both concluded that in a comparison of a number of interpolation routines, the multiquadric technique was the best (1984, p. 368). Using both real and mathematical data, the authors concluded that the multiquadric technique was a good method of interpolation using this data set and that the cone model gave the best results (Schiro and Williams 1984).

Franke (1982) compared a number of interpolation routines evaluating the following parameters: accuracy, visual aspect, timing, storing requirements and ease of implementation. The author generated 6 mathematical surfaces and used 3 different sampling densities - 100 points, 33 points and 25 points to test the routines. Franke (1982) concluded that the multiquadric technique was the best of the global interpolation routines.

A series of figures presented in the Franke (1982) paper shows the multiquadric test surfaces based on the 3 sampling densities and the original test surface. The test surface consisted of two peaks one higher than the other with a valley in between and a depression area located adjacent to these highs. The multiquadric surface based on 100 points was visually the same as the test surface. The surfaces based on 33 and 25 points were similar to the test surface in depicting the highs, but did not predict the saddle.

### **1.3 APPLICATIONS TO FLUID SPEEDS IN A RIVER**

Saunderson (1992), using the data of Brooks (1985) interpolated fluid speeds in a river using the cone model (i.e.  $C=0$  in equation 4). Saunderson (1992, 1994a) wrote a series of C programs to generate a multiquadric surface and to plot the interpolated fluid speeds.

The river used in this initial study (Brooks, 1985) was the Nottawasaga River, a sand bed river in southern Ontario,

near the Town of Angus. The relative roughness of the Nottawasaga River was small (i.e. the  $d(\text{depth})/D_{50}$  (average particle size) was less than 1). Fluid speeds were sampled at a number of verticals across the channel; the number ranged from 6 to 8. In the vertical, speeds were collected at points every 0.20 m below the surface, starting at a point 0.05 m below the surface (Brooks, 1985).

This study (Saunderson, 1992) was the first to apply Hardy's (1971) multiquadric technique to fluid speeds in a river. Most of the other studies (e.g. Hardy, 1971; Shaw and Lynn, 1972) produced contour maps based on the interpolated data. This required the interpolated data to be fitted to a grid of some sort and either manual or computer produced contours drawn based on interpolations derived from the contouring procedure. Saunderson (1992) avoided the need for this second interpolation and contouring by plotting the speeds using a colour class system in which each class represented all speeds as a percentage of the maximum speed.

Saunderson (1992) wanted to investigate the use of the multiquadric technique of interpolation to river fluid speeds, which is an irregular surface. Previous studies (e.g. Shaw and Lynn, 1972) had demonstrated the effectiveness of the multiquadric procedure for other irregular surfaces. Saunderson (1992) was concerned with the visual display of fluid speeds based on the surface generated by the multiquadric procedure.

.

Saunderson (1992) concluded that the multiquadric technique of interpolation could be applied to fluid speeds and that the cone model accurately reproduced the known points. Further, it was concluded that the distribution of the interpolated speeds was "intuitively accurate" (1992, p 192). Saunderson (1992) visually examined the fluid speed patterns based on the interpolated points and did not identify any error associated with the procedure and the application.

There is a need to identify the magnitude of error associated with the multiquadric technique of interpolation and fluid speeds; this distribution of these errors and causes of these errors. This current study will focus on the errors related to the application of the multiquadric technique to fluid speeds from a gravel bed river.

The current study uses the procedures and computer programs of Saunderson (1992, 1994a), but differs in many key aspects.

- (1) The river used has a gravel bed and small depth (i.e. high relative roughness);
- (2) The sampling density of fluid speeds is higher than in the Brooks study;
- (3) The errors associated with the multiquadrics will be quantified;
- (4) Relationships between geomorphological variables (relative roughness and turbulence) and errors will be established.

#### **1.4 GOAL AND OBJECTIVES**

The goal of this thesis is to test the multiquadric



technique of interpolation using a fluid speed data set sampled from Big Otter Creek, Ontario, a shallow, wide, gravel bed river.

The objectives of the thesis are:

- (1) to test the multiquadric technique of interpolation using fluid speeds from a gravel bed river (Chapter 3);
- (2) to identify the magnitude and distribution of errors involved with this technique (Chapters 4 and 5);
- (3) to identify patterns of errors, if any (Chapters 4 and 5);
- (4) to identify geomorphological explanations for these errors (Chapter 5);
- (5) to evaluate a sampling procedure used to examine fluid speeds in a river (Chapter 5).

## CHAPTER 2: STUDY AREA AND FIELD METHODOLOGY

### 2.1 STUDY AREA

An approximately 500 meter long reach of Big Otter Creek in south-western Ontario was selected for the study area. The selected reach is located in the town of Otterville, off Highway 19, between the towns of Norwich and Delhi, south of Woodstock (Figure 2.1a). This area was selected because of the accessibility and because the bed material, channel width and depth were different than that of Saunderson (1992).

Big Otter Creek and its tributaries drain an area of 697 sq. km (Environment Canada). The length of the river from its source near New Durham to Port Burwell, where it enters Lake Erie is 48 miles [77 km] (Chapman and Putnam, 1984).

The drainage basin has 2 main physiographic features - a sand plain and morainic ridges. The Norfolk Sandplain is located in the south-southeast area of the basin and the Mount Elgin Ridges are located in the north-north east (Sibul, 1969). Prior to Otterville, Big Otter Creek and its tributaries flow through areas of morainic, outwash, fluvial and lacustrine deposits of Wisconsinan age and alluvial deposits of Pleistocene age (Sibul, 1969; Chapman and Putnam, 1984). The river bed in the study reach consists of alluvial material in the coarse sand to boulder size ranges.

FIGURE 2.1A LOCATION OF STUDY AREA

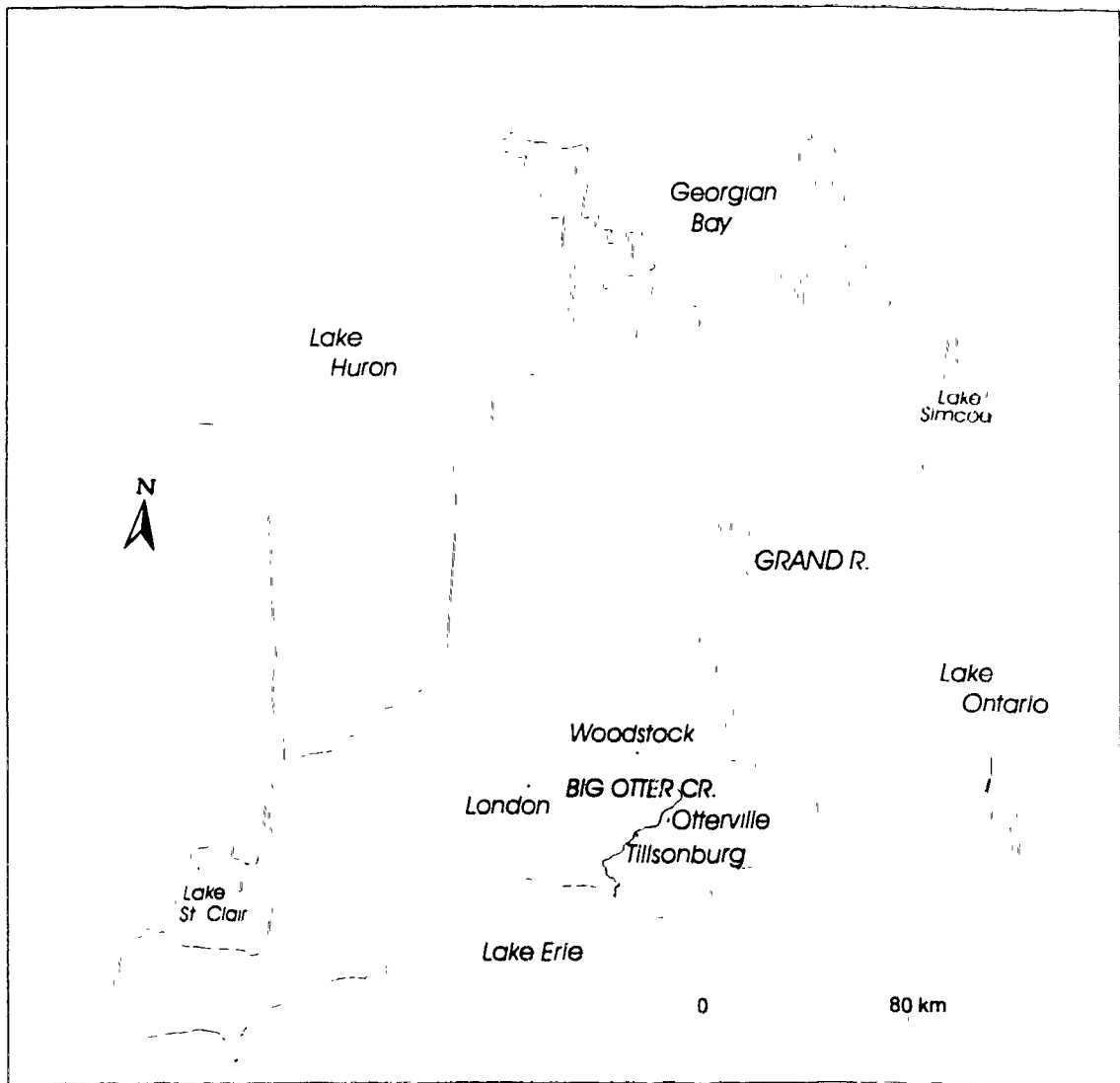
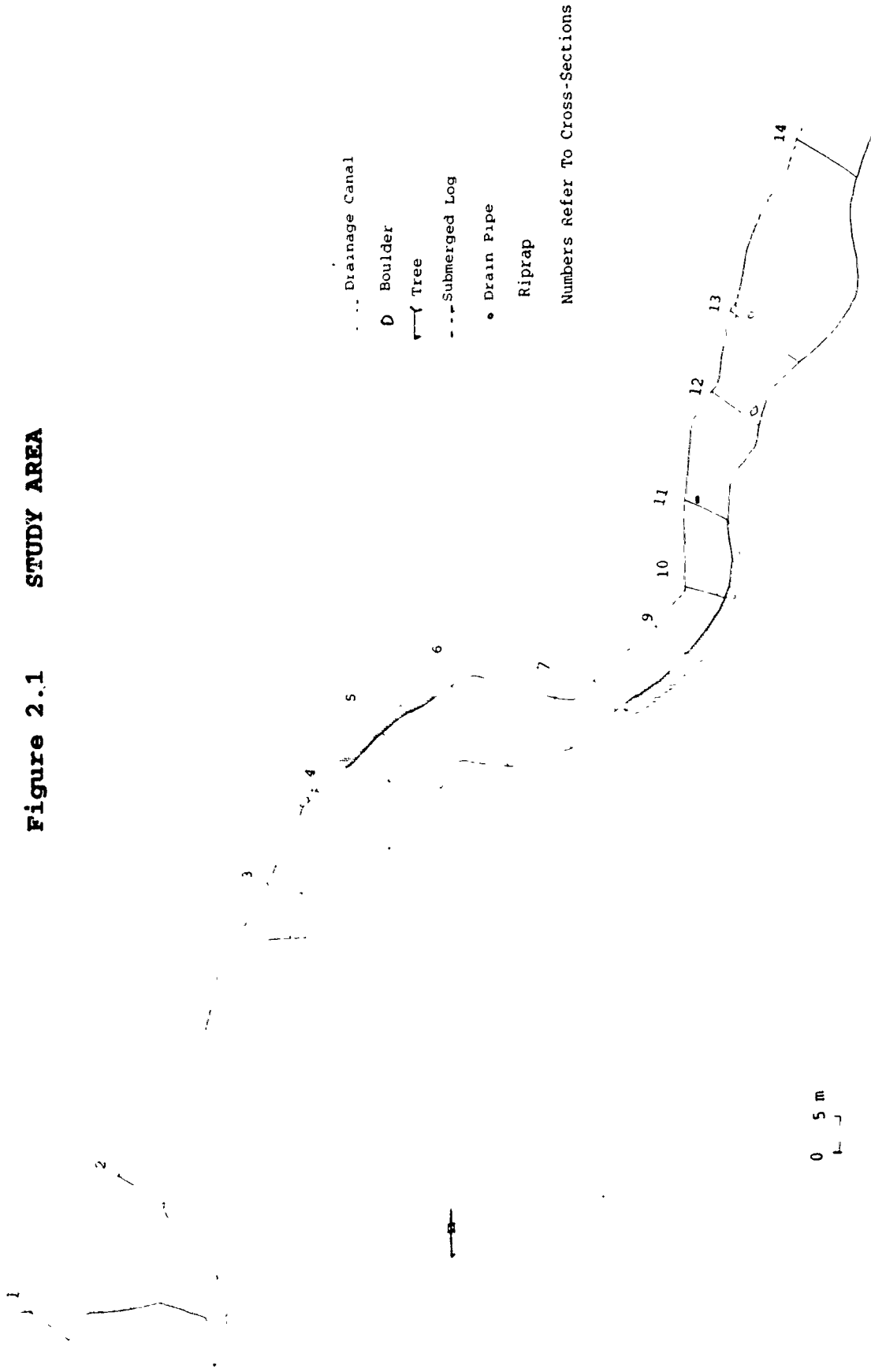


**Figure 2.1**      **STUDY AREA**



## 2.2 COLLECTION OF FIELD DATA

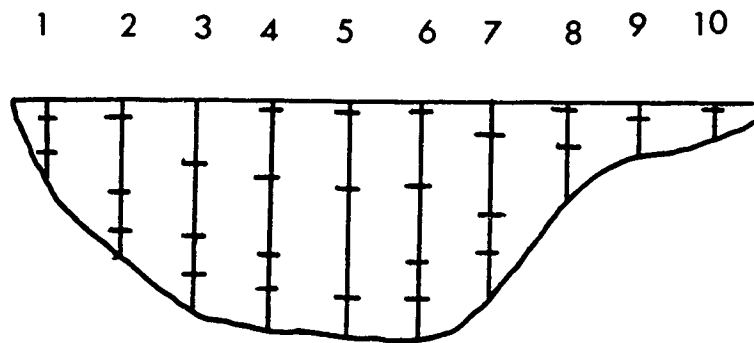
A total of 14 cross-sections, or transects, were selected throughout the study reach (Figure 2-1b) and labelled CS1 to CS14 starting with the most upstream transect. Each cross-section was marked in the field by placing either an 8 inch metal spike or surveyor's pin in each bank. Prior to the selection of the 14 transects, a visual survey of the area was completed and locations of potential influences on fluid speed (e.g. inchannel obstructions, change in bed morphology and differences in bed roughness) were noted. The location of the transects was based on an attempt to sample the different areas of the river as they relate to fluid speeds; for this reason, the meander unit was more densely sampled.

At each of the 14 sections a transect line was strung across the channel. The upstream left (UL) water's edge was marked on this line using masking tape. This UL marker served as a reference point from which channel and panel widths were measured. The wetted width of the transect was measured using a 30 m tape. The distance between the upstream left water's edge and upstream right water's edge was considered the wetted width.

Each transect was divided into 10 panels or verticals (Figure 2.2) using the equal width method (Water Survey of Canada, 1986). The midpoint of each panel was marked on the transect line and identified as P1 to P10 beginning at the panel closest to the UL marker. At each panel the depth was

measured using a meter stick. In instances where there were large particles beneath the transect line, the depth was measured to the top of the particle. No bed material was removed during the collection of depth and speed data.

**Figure 2.2 SCHEMATIC OF TRANSIT DIVISION FOR A CROSS-SECTION LOCATED IN THE MEANDER**



The numbers refer to panel or transect numbers, which start from the upstream left side (1) and increase across the channel. Dash mark denote the position in the vertical where fluid speed was measured - the first position was 0.025 m off the bed followed by 0.05 m, 0.10 m and 0.15 m off the bed. After the near bed reading (i.e. 0.25 m off the bed), fluid speeds were measured starting at 0.05 m off the bed and every 0.05 in the vertical. Figure is not to scale.

Fluid speed measurements were taken at specific points in the vertical starting at a point 0.025 m above the bed (this

was the minimum depth at which the current meter probe could measure speed). Subsequent measurements were taken every 0.05 m, beginning at 0.05 m off the bed, i.e. 0.025 m, 0.05 m, 0.10 m etc. off the bed. Speed measurements were taken with a Marsh McBirney 201D portable electromagnetic current meter. Ten fluid speeds were collected for each point in the vertical and later averaged to give the time averaged speed at that position. The technique of dividing the channel into panels, and sampling at various positions in these verticals has been used in a number of studies examining fluid speed patterns and river sedimentology (eg. Jackson, 1975; Bridge and Jarvis, 1977; Hickin, 1978; Robert *et al.*, 1992).

During the two week sampling period there were no precipitation inputs into the basin; also, there was no measurable change in the stage of the river over the sampling interval. It was assumed that there were no changes to the fluid speed patterns over the time of sampling.

Table 2.1 summarizes the width, average depth and average fluid speeds for all 14 cross-sections. The widest sections (12-14) are in the area downstream of the bend unit. Cross-section 7 has the smallest mean depth and the fastest average fluid speed and is located in the straight area between the 2 bends.

Bed material was also sampled at each cross-section using 2 methods. In the first method, bed material was sampled using a hand held scoop. The scoop was dragged across the bed

collected material throughout the panel. Careful attention was paid so that the finest material was included in this sample. Initially, one sample per panel per cross-section was collected, but this procedure was later modified so that only representative samples from each cross-section were taken. If the bed appeared to be uniform, one sample was taken; if the material varied across the channel, two or three samples were collected to represent the various areas of the bed. Given the nature of the bed material in the study reach, the results of the bed material sampled for cross-sections 8 to 14 are comparable to the material for sections 1 to 7.8

**TABLE 2.1 SITE SUMMARY**

Cross-Section #	Width (m)	Mean Depth (m)	Mean Fluid Speed (m/sec)
1	10.20	0.25	0.21
2	9.87	0.22	0.28
3	11.45	0.30	0.19
4	13.45	0.17	0.34
5	15.03	0.18	0.28
6	12.30	0.16	0.44
7	10.75	0.15	0.53
8	7.55	0.25	0.32
9	7.51	0.24	0.24
10	8.57	0.30	0.21
11	7.39	0.22	0.38
12	10.50	0.22	0.26
13	16.20	0.24	0.21
14	11.80	0.29	0.26



Each scoop sample was placed in a zip lock bag, labelled and transported back to the laboratory. In the laboratory the samples were dried and sieved using a Ro-tap sieve shaker. The sieve stack started at -6 phi and decreased by 1 phi units until 0 phi; then the size decreased by half-phi units. The last sieve used was +4 phi, with the pan representing material finer than this.

The second method was used to sample the macro-scale roughness elements. This consisted of material in the cobble to boulder size ranges. Five particles per panel per cross-section were collected off the bed (where possible) and their long, intermediate and short axes were measured to the nearest 0.5 centimetre. The particles that were measured were resting on the surface of the bed and were not buried in the channel. These particles were then placed back on the bed.

### **2.3 PARTICLE SIZE AND DISCUSSION**

A total of 72 scoop samples were collected and analyzed. One sample per panel was taken CS1 to CS7; 2 samples were taken at CS8-CS12 and 3 samples were collected at both CS13 and CS14. No samples were analyzed at panels 1 and 9 at CS 1 or at panel 4, CS 2 because the samples became contaminated during transport back to the lab. No samples were collected at panel 10, CS 5 because of the nature of the bed material. The bed in this area consisted of boulder size material, which was too large to be collected by the scoop.

These samples were statistically analyzed for median particle size, graphic mean, inclusive graphic standard deviation and graphical skewness (Boggs, 1987). Table 2.2 summarizes the graphic means for each transect.

The standard deviation can be used to describe the sorting of the sampled material (Boggs, 1987). The bed is made up mostly of poorly sorted material in the pebble size class range. One of the samples had a value of 0.47  $\Phi$ , indicating that it was well sorted, while 12 samples, including all of the samples downstream of the meander unit (CS12 to CS14) were extremely poorly sorted.

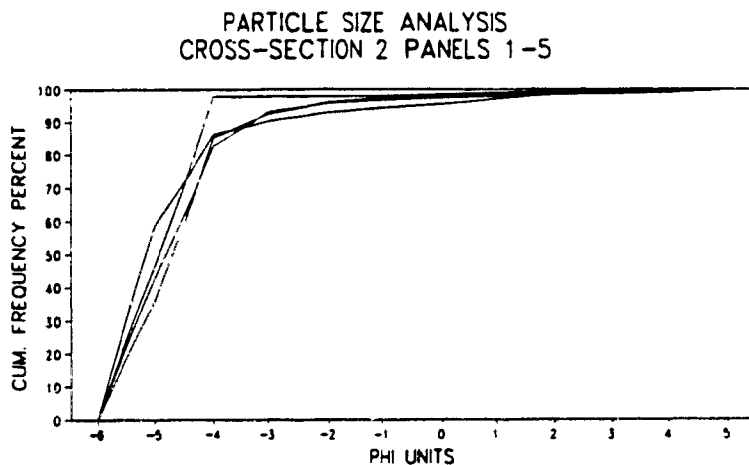
**TABLE 2.2 GRAPHIC MEAN (PHI UNITS  $\Phi$ )**

	P1	P2	P3	P4	P5	P6	P7	P8	P9	P10
CS1		-4.89	-5.40	-5.17	-5.40	-5.19	-5.40	-4.07		2.33
CS2	-4.95	-5.00	-4.79		-4.79	-4.97	-4.77	-4.48	-4.68	-4.88
CS3	-0.65	-6.62	-4.78	-4.78	-4.83	-4.88	-4.72	-5.00	-5.03	-5.00
CS4	-3.87	-4.65	-4.88	-3.01	-4.81	-4.60	-4.99	-5.02	-4.92	-5.79
CS5	-4.57	-5.49	-5.11	-4.53	-6.40	-4.75	-4.70	-5.99	-4.67	
CS6	-3.69	-3.98	-4.67	-5.08	-4.82	-4.93	-5.75	-4.60	-4.00	-4.72
CS7	1.45	-3.03	-3.45	-5.92	-5.02	-4.72	-3.85	-4.60	-4.83	-5.30
CS8					-5.25				0.53	0.59*
CS9				-5.33					-2.29	
CS10						-5.40			-2.93	
CS11				-5.03						-2.00
CS12		-2.38						-2.97		
CS13		-1.19				-2.87				1.76
CS14		-4.21				-4.50				-2.92

\* At CS 8 no sample was taken at panel 10. One sample at panel 9 was collected and split. The value presented under the headings panel 9 and panel 10 represent the mean for runs 1 and 2 respectively of the sample from panel 9.

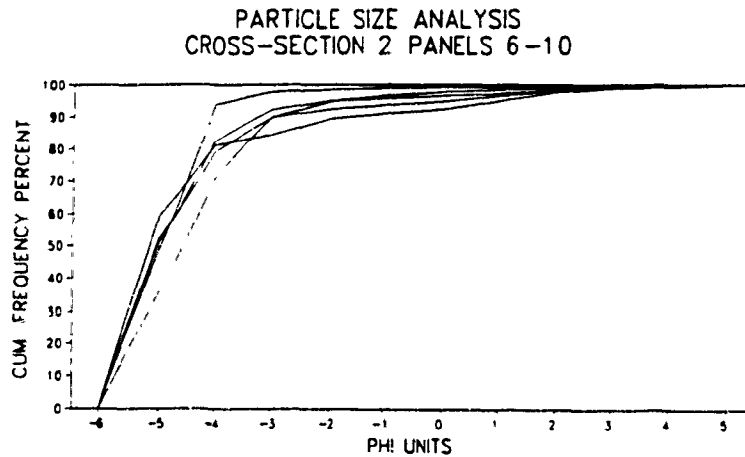
For CS1 to CS7 the sampled bed material was comprised predominantly of medium to large size pebbles and small size cobbles (size according to the Wentworth scale). There were, however, areas of the bed that were comprised of finer material, ie. sand size, - panel 10 at CS 1 (fine sand); panel 10, CS 3 (coarse sand) and panel 1, CS 7 (medium sand). Figure 2.3 is a typical set of cumulative frequency percent curves for sections 1 through 6. There is little variation in particle size range across the channel and between the cross-sections. Cross-section 7. shows a greater degree of variability in panels 1-5, but then shows the similar patterns as the curves for sections 1-6 in Figure 2.3.

**FIGURE 2.3A PARTICLE SIZE ANALYSIS CROSS-SECTION 2 PANELS 1-5**



Note the consistency in the range of particle size across the channel.

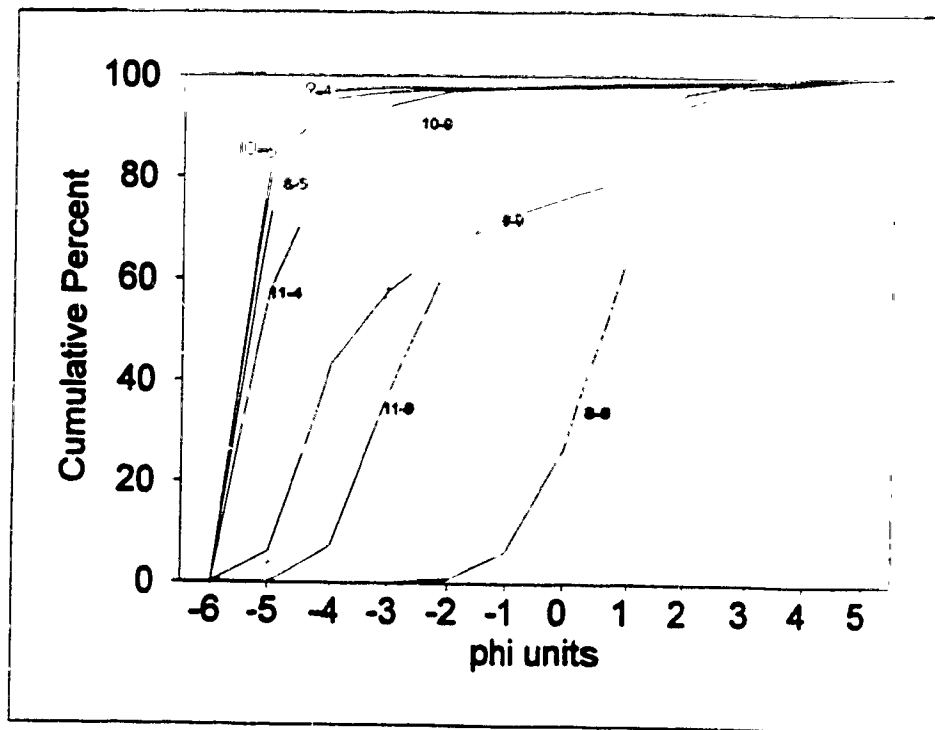
**FIGURE 2.3B PARTICLE SIZE ANALYSIS CROSS-SECTION 2 PANELS 6-10**



Note the consistency in the range of particle size across the channel.

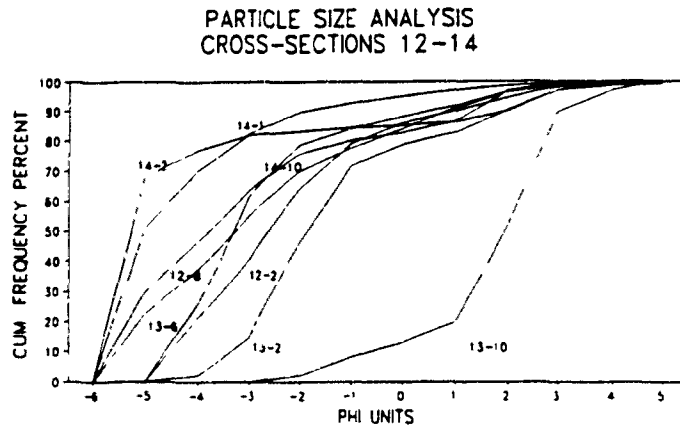
Figure 2.4 shows the cumulative frequency curves for transects numbered 8 through 10. From the curves and table 2.2, there appears to be two zones of material in this section of the reach - i) cobble sized material and ii) granule size. The larger cobble size material was located in areas on the outside of the meander, while the smaller size material was located at points along the depositional bar.

FIGURE 2.4 PARTICLE SIZE ANALYSIS CROSS-SECTIONS 8-11



Cross-sections 12 and 13, in the area downstream of the meander unit (Figure 2.1b) have bed material consisting mostly of granule to small pebble sizes. Panel 10 at CS 13 had medium sized sand material on the bed. The last cross-section of the study reach, CS14, has an average scooped particle size that was larger than the other 2 cross-sections in the region downstream of the meander unit. The particles are in the large pebble size fractions (Figure 2.5).

**FIGURE 2.5 PARTICLE SIZE ANALYSIS CROSS-SECTIONS 12-14**



#### **2.4 INTERPRETATION OF SEDIMENT CURVES**

The shapes of the curves in Figures 2.3 to Figure 2.5 is due to the weight of the individual size fractions in each sample. For the curves representing the panels at CS2, and for the panels located along the outside of the bend (Figure 2.3), the majority of the weight of the sample comes from a few particles in the coarsest class size (ie. -6, -5, and -4

phi range). As a result, the cumulative percent is very large in these coarse size fractions, giving rise to the steep slope on the graphs in this area.

Variations in particle size can be explained in terms of fluid speed patterns. Cross-sections 8-11 are in the bend area. The depth is greater along the outer regions of the meander in the pool area, while across the point bar along the inner bank depths are smaller. Fluid speeds are greatest along the outer bank of a meander and lowest along the inside (Leopold et al. 1963). As a result, material is deposited along the inner side, while the pool is an area of erosion.

The sand size material at CS3 and CS13 were in areas where there were inchannel obstructions. Upstream of 3 there was an inchannel vegetation jam that created an area of lower speeds in the downstream zone. This zone of lower speeds, could result in the deposition of material that was being transported. At CS 13, there was a submerged log beneath the transect which extended from the bed through panel 10. The bed material in this area was all sand size. This log obstructs flow, resulting in a decrease which can result in the deposition of material (Hjulstrom, 1935; Sundborg, 1967).

The channel widens out at CS 7. Panel number 1 was located in an 'alcove'. This area was a zone of nearly still water (average fluid speed at the time of sampling was -0.007 m/sec). The bed material in this section of the channel consisted of fine sands and silt.

## 2.5 MEASURED PARTICLE RESULTS

Figure 2.6 displays the distribution of the intermediate axis for the 630 measured particles; Figures 2.7 to 2.9 show the average intermediate axis of the measured particles for each panel at each cross-section. The numbers on the side of Figures 2.7 to 2.9 refer to panel numbers.

**FIGURE 2.6 DISTRIBUTION OF PARTICLE SIZE (MEASURED B AXIS)**

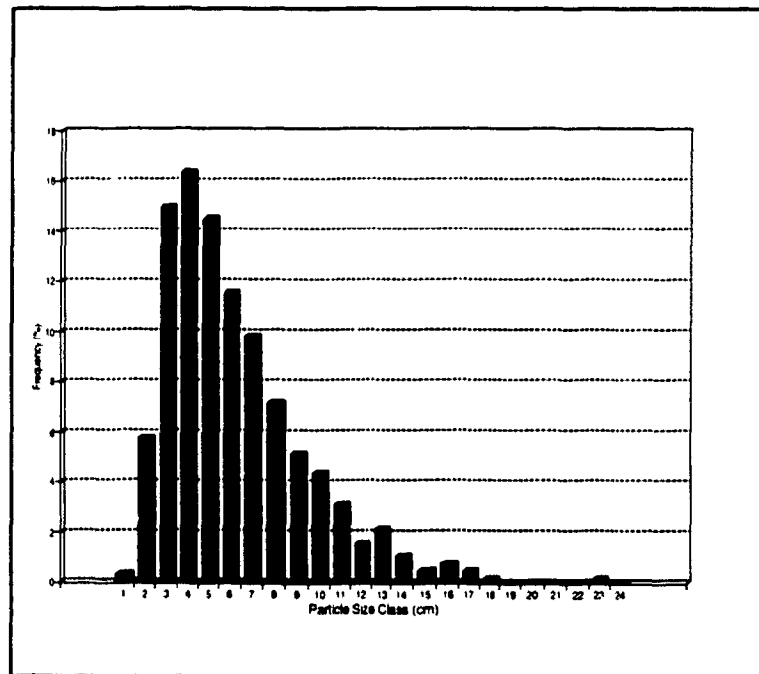




**FIGURE 2.7 AVERAGE MEASURED PARTICLE SIZE CROSS-SECTIONS 1 TO 5**

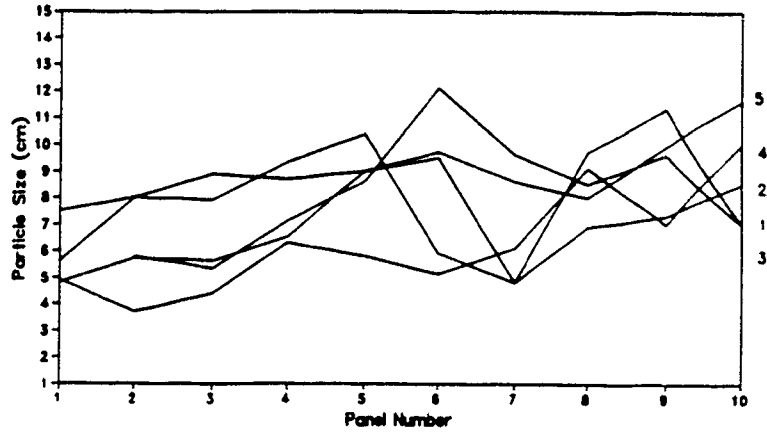


**FIGURE 2.8 AVERAGE MEASURED PARTICLE SIZE CROSS-SECTIONS 6 TO 11**

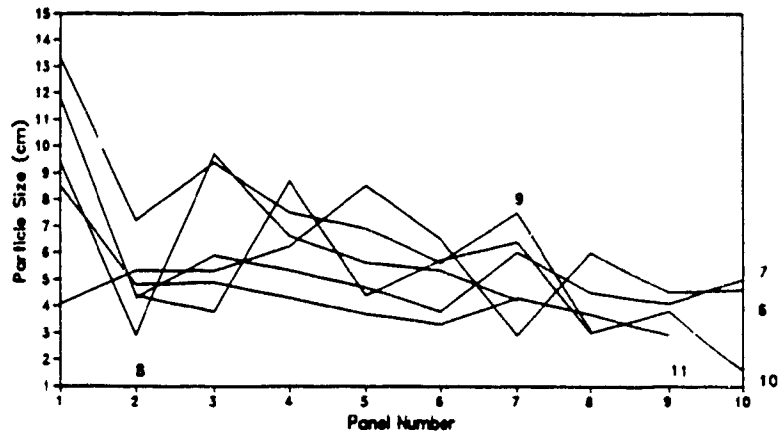
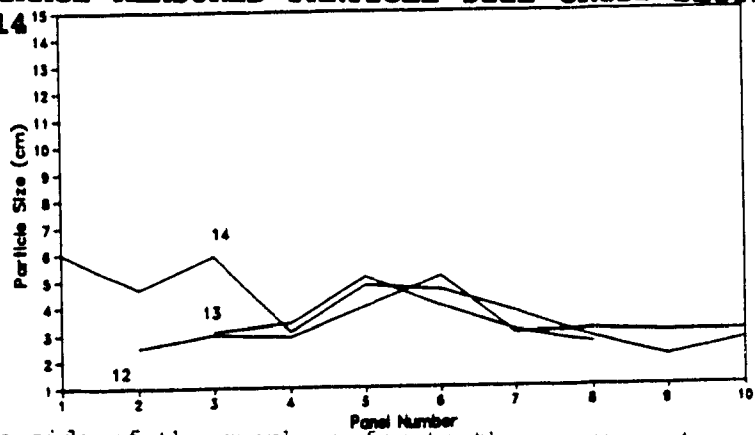


**FIGURE 2.9 AVERAGE MEASURED PARTICLE SIZE CROSS-SECTIONS 12 TO 14**



The number at the side of the graphs refer to the cross-sections.

From Figure 2.6 it can be seen that the average intermediate axis ranges from 1 cm to 23 cm. The measured particles are concentrated in the size ranging from 3 cm to 8 cm, with particles from 4.0 to 4.9 cm being the modal class.

From figures 2.7 to 2.9 it can be seen that there is variation in average intermediate axis across the channel and throughout the study reach. For CS1 to CS5 there is a general increasing trend in average particle size across the channel, starting at the upstream left (Figure 2.7). Cross-sections 8 to 11 (Figure 2.8) show a decreasing trend in average intermediate axis across the channel. The largest particles were located along the outside of the bed. Some of the particles sampled in the region closest to the outer bank in these cross-sections may have been part of the riprap used to stabilize the bank (Figure 2.1b for the locations of the riprap). No samples were collected at panel 10, CS8, CS9 or CS11 because of the nature of the material. These panels were over the point bar, and the material comprising this feature was too small to measure (see the curves in Figure 2.4 as to the type of material found in this area of the reach). Cross-section 7 shows little variation in the range of particle size across the channel. Cross-sections 12 to 14 show less variation in the range of average intermediate B axis (Figure 2.9). The average measured particles in this section of the reach are smaller than the material in the upstream areas, ie. CS1 to CS11 (compare the curves in Figure to 2.9 to those in

2.8 and 2.7).

## 2.6 SUSPENDED SEDIMENT AND TEMPERATURE

One suspended sediment sample and one temperature reading were taken and recorded for each of the 14 transects. This data was needed to calculate the Reynolds number (discussed in chapter 5). The suspended sediment sample collected was a depth integrated sample. Table 2.3 summarizes the results of the suspended sediment concentrations and temperature readings.

**TABLE 2.3 SUSPENDED SEDIMENT CONCENTRATIONS AND TEMPERATURE**

X-Sect	Sed/Lit re mg/L	Temp. (oC)
1	8.90	12.0
2	50.81	12.0
3	15.32	12.0
4	22.07	10.0
5	19.91	11.0
6	15.36	11.0
7	10.40	12.0
8	12.13	9.0
9	3.93	10.0
10	13.58	10.0
11	11.28	10.0
12	11.51	11.0
13	18.64	11.0
14	30.45	11.0

## **2.7 BED LOAD SAMPLING**

Bed load transport could have an influence on the distribution of speeds in the river. The movement of material could create local areas of fluid acceleration and deceleration, as well as influence the type of the material on the bed. To examine bed load transport two bed load samples were collected using a Helley-Smith type bed load sampler. The sampler was placed on a flat area of the bed at a position just downstream of CS2 and at CS7 (Figure 2-1b).

The only material that was captured with the sampler was organic debris - leaves and small twigs. After drying, some fine silt did appear to be visible on some of the leaves. Although the sampler was placed on a flat portion of the bed, there were places where the bottom of the sampler opening was not in contact with the bed. Although no movement of bed material was visible, it is possible that particles that were moving as bed load did not get collected because of the lack of contact between the sampler and the bed.

## CHAPTER 3: TESTING THE MULTIQUADRIC TECHNIQUE

### 3.1 INTRODUCTION

Saunderson (1992) used the cone model (ie.  $C=0$  in equation 4), which, in matrix form, is:

$$(6) \quad \begin{bmatrix} 0 & | & p_1-p_2 & & & | & p_1-p_n \\ | & p_2-p_1 & & 0 & & & | & p_2-p_n \\ \vdots & & & & & & & \\ | & p_n-p_1 & & & & & & 0 \end{bmatrix} \begin{bmatrix} c_1 \\ c_2 \\ \vdots \\ c_n \end{bmatrix} = \begin{bmatrix} z_1 \\ z_2 \\ \vdots \\ z_n \end{bmatrix}$$

and in algebraic form:

$$(7) \quad A \cdot b = X$$

with a solution of:

$$(8) \quad b = XA^{-1}$$

Here, A uses the x,y coordinates of width and depth; X is the sampled fluid speed (z) and b is a solution set of unknown coefficients. From the matrix,

$$(9) \quad |p_1-p_n| = [(x_1-x_n)^2 + (y_1-y_n)^2]^{1/2}$$

and

$$(10) \quad \sum_{j=1}^n c_j [(x_1-x_j)^2 + (y_1-y_j)^2]^{1/2} = z_1$$

where  $x_j$  and  $y_j$  are the cartesian coordinates of the vertex of each cone,  $z_j$  is the speed at those coordinates and  $c_j$  is the coefficient. After a multiquadric surface has been generated, a new fluid speed,  $z_p$ , at points  $x_p, y_p$  is determined by:

$$(11) \quad \sum_{j=1}^n c_j [(x_p-x_j)^2 + (y_p-y_j)^2 + c]^{1/2} = z_p$$

The only unknown in this equation is the coefficients,  $c_j$ .

Matrix algebra is used to solve for these coefficients. Saunderson used the singular value decomposition, and as back-up, the Gauss-Jordan routines of Press et al. (1988).

Saunderson (1992, 1994a) wrote a C-program to generate a series of new  $x,y$  pairs which were used in equation 10 ( $x_p, y_p$ ) to generate a complete surface of fluid speeds. To display the results, Saunderson used a colour class scheme based on percentage of the maximum speed (see his figure 2 (1992) and figures 1-3 (1994a)). In the plotting package, the bed was defined and areas below the bed were coloured out. This allowed for the presentation of fluid speeds for an entire cross-section, including the bed topography.

### **3.2 COMPUTER PROGRAMS**

A series of 4 programs, 3 by Saunderson (1994) and 1 by Press et al. (1988) were used in this thesis to interpolate and plot fluid speeds. These programs were run on a Microsoft Quick C compiler. The large and huge memory modules in the compiler were used in compiling the programs. Initially, only the large module was used, but for the larger data sets, the huge module was required.

The first program, `matrx1.c` reads in 2 input files - `xy.dat` (table 3.1) and `z.dat` (table 3.2). These 2 files are the coordinates (`xy.dat`) of the sampled fluid speeds (`z.dat`). The collection of data for these 2 files is described in

Section 1.3. This program calculates the square roots of equation 9, which are printed along with the original sampled fluid speeds ( $z_j$ ) to an output file called `matrx1.dat`. `Matrx1.dat` is used by the singular value decomposition (SVD) routine of Press et al. (1988) to solve for the unknown coefficients ( $c_j$ ). Table 3.3 is a sample of the output file from `matrx1.dat` and table 3.4 is from the file `CVEC`, which is the output from the SVD program.

The `CVEC` file provides a check of the solution of coefficients by multiplying the solution vector by the original matrix (table 3.4). It will be noted that there is some discrepancy between the original values and the solution times (\*) matrix values. The difference is generally in the 5<sup>th</sup> or 6<sup>th</sup> decimal place and is the result of computer rounding.

The original `xy`-data (table 3.1) and the solution vector (`CVEC`, table 3.4) are read by the program `xyzpart.c`. This program will generate new coordinates (equation 10) by decreasing from the abscissa by 0.01 m in the X direction and 0.05 m in the Y direction. Using these new  $x_p$  and  $y_p$  coordinates and the solution vector (`CVEC`) new fluid speeds are interpolated using matrix algebra.

**TABLE 3.1 XY.DAT**

-0.37	-0.03
-1.11	-0.01
-1.11	-0.11
-1.85	-0.03
-1.85	-0.13
-2.59	-0.03
-2.59	-0.13
-3.33	-0.005
-3.33	-0.105
-3.33	-0.18
-4.07	-0.055
-4.07	-0.155
-4.07	-0.23
-4.81	-0.07
-4.81	-0.17
-4.81	-0.245
-5.55	-0.085
-5.55	-0.185
-5.55	-0.285
-6.28	-0.025
-6.28	-0.125
-6.28	-0.225
-6.28	-0.325
-7.02	-0.04
-7.02	-0.14

**TABLE 3.2 Z.DAT**

0.303
0.544
0.453
0.567
0.413
0.662
0.461
0.487
0.548
0.282
0.605
0.419
0.189
0.621
0.467
0.08
0.523
0.309
0.072
0.49
0.464
0.295
0.238
0.218
-0.001

Table 3.1 X is the distance of a panel, in metres, from the upstream left used in the cross-section analyses. Y is the depth below the surface in metres also used in the cross-section analyses.

Table 3.2 is the fluid speed in metres per second (m/sec). In the cross-section analyses, this value is average of the 10 sampled speeds. In the plan view analyses, the speed is the averaged bed and surface speed, or it is the average of all points in the vertical.



### TABLE 3.3 OUTPUT FROM MATRX1.DAT

Matrix for input to xsvbksb.exe  
Size of matrix, number of solutions  
30 1  
Matrix  
0.000000 0.752396 1.510008 1.512985 . . .  
0.752396 0.000000 0.762775 0.760805 . . .  
1.510008 0.762775 0.000000 0.100000 . . .  
  
.  
.  
.  
.  
.

Solution vector (r.h.s.), z values:  
-0.0180 -0.0240 0.0090 0.0000 0.0020

Matrx1.dat - output from matrx1.c. This is used as input for programs from Press et al (1988) which is used to create the data file cvec (table 3.4).

### TABLE 3.4 CVEC OUTPUT

Vector number 1  
solution vector is:  
0.164384 -0.372281 0.222626 -0.546791 0.604625  
-0.870046 0.692436 0.686079 -2.063146 1.536635  
-0.656949 -0.604115 1.209920 -0.482458 -1.809983  
2.282702 -0.738284 -0.102624 0.948756 0.035493  
-0.735308 0.530097 -0.137827 -0.799575 1.057251

The solution vector is the result of the singular value decomposition (SVD) used to solve for the unknown coefficients in equation 4.

original right-hand side vector:  
0.303000 0.544000 0.453000 0.567000 0.413000  
0.662000 0.461000 0.487000 0.548000 0.282000  
0.605000 0.419000 0.189000 0.621000 0.467000  
0.080000 0.523000 0.309000 0.072000 0.490000  
0.464000 0.295000 0.238000 0.218000 -0.001000

The original right-hand side vector is the original fluid speed data in metres per second.

(matrix)\*(sol'n vector):  
0.303003 0.543995 0.453000 0.567000 0.413000  
0.662001 0.461001 0.487002 0.548002 0.282002  
0.605002 0.419002 0.189002 0.621002 0.467002  
0.080001 0.523002 0.309002 0.072002 0.490001  
0.464002 0.295002 0.238002 0.218002 -0.000999

This represents a check of the accuracy of the solution vector. The (matrix)\*(sol'n vector) should be the same, or very close to the original right-hand side vector (above).

Saunderson's xyzpart.c program was modified for the current application in 2 main ways. First, the original

program calculated the partial derivatives. Since these were not used in this study, the program was modified to calculate and print only the new fluid speeds. This step decreased processing time and reduced the amount of computer storage space needed to store the output files. Secondly, new x and y values were generated by decrementing x and y by 0.01 and 0.001 m, respectively in the cross-section analyses and by 0.10 cm in the plan view analyses. This increased density was needed in order to locate all original data points.

To display the results, Saunderson (1992, 1994) used a colour class scheme. The 10 classes were based on fluid speed as a percentage of the maximum speed. The class intervals used were (1)  $\geq 95\%$  of the max.; (2)  $\geq 90\%$  and  $< 95\%$  of the max.; (3)  $\geq 85\%$  and  $< 90\%$  of the max. and so on changing by 5% intervals until the last class, which consisted of all speeds  $> 0\%$  and  $< 55\%$  of the maximum. The class intervals selected were arbitrary; however the number of classes is limited to the number of colours that can be displayed.

### **3.3 TESTING THE METHODOLOGY**

#### **3.3.1 INTRODUCTION**

In order to achieve the goal and objectives of the thesis, known points - xy coordinates and the corresponding sampled fluid speeds at those coordinates - were removed from

the data set to create a smaller subset of input data which was then used in the computer programs described above. The interpolated speeds generated using the subset were then compared against the known speeds from the complete data set. This procedure is similar to that used by Tabios and Salas (1985) in their application of multiquadrics to rainfall data.

Due to the overall size of the data set involved, and the amount of time and computer space needed to process and store the information, and because of the number of analyses performed (tables 3.5 and 3.6) only cross-sections 8 to 11 were used in the cross-section analyses of the errors and sections 7 to 11 were used in the plan view analyses of the errors.

To determine the influence that the number (density) of control points and their distribution had on the effectiveness of the interpolation, two methods of control or input point selection were used. The subset of input data was created by systematically and randomly removing points from the complete data set. The absolute and relative errors were then calculated for both types of control point selection.

The general procedure used to evaluate the multiquadric technique of interpolation was:

- (1a) conversion of field data (cross-section);
- (1b) generation of plan view grid;
- (2) creation of subset of input data;
- (3) execution of C-programs;
- (4) calculation and graphing of errors.

### **3.4 TESTING PROCEDURE**

#### **3.4.1 CONVERSION OF FIELD DATA (CROSS-SECTION ANALYSES ONLY)**

The xyzpart.c program generated new points starting at 0,0 and decrementing to the left and downwards. This means that all the xy coordinates have negative values (see table 1 in Saunderson, 1994). The field data for this study were collected at a point starting at the left hand side of the channel and upwards from the bed (chapter 2). This meant that either the program had to be modified to suit the data, or the data needed to be modified to accommodate the program.

The field data were converted to suit the program. The x coordinate was changed to reflect the new starting point and the y coordinate was converted to values below the surface (table 3.1). The fluid speeds did not need to be converted.

#### **3.4.2 GENERATION OF PLAN VIEW GRID**

Cross-sections 7 to 11 were used to examine the magnitude and distribution of errors in plan view form. A 40 cm by 32 cm grid was placed over the area of the map encompassed by CS7 to CS11 (the map used in this analyses had a smaller scale than the one in Figure 2.1b). This centimetre grid was divided into 10 units (millimetres) and the location of each of the panels at the 5 cross-sections was identified and

recorded. These XY coordinates were then used, along with the bed, surface and average fluid speeds, as input for the multiquadric system of equations.

### **3.4.3 SELECTION OF CONTROL POINTS**

#### **3.4.3.1 SYSTEMATIC REMOVAL OF POINTS - CROSS-SECTION**

The systematic removal of points can be grouped into 2 categories: in the first a single value was removed (SVR) from the data set so that no two adjacent points in a vertical were removed (examples of SVR include the removal of every odd, even, third point etc.). In the second category, entire panels or verticals were removed. Table 3.5 summarizes the systematic removal of points for cross-sections used in the testing procedure. The systematic removal of points was undertaken to determine the role that the density and location of the points have on the interpolants.

Within the two categories of systematic removals, two divisions can be made. For rows 1 to 10 any point, including those at panels 1 or 10 were removed. This meant that those points that were located along the convex hull, i.e. points at the bed or surface, were removed to create the subset. In the second division, the points along the convex hull were not removed from the analysis (rows 11 to 19). The objective of these two types of analysis was to determine the influence

that the removal of points along the convex shell of the data set would have on the quality of interpolated values.

**TABLE 3.5 SUMMARY OF SYSTEMATIC REMOVAL OF POINTS - CROSS-SECTION ANALYSES**

	Type of Analysis	Cross-Section 8	Cross-Section 9	Cross-Section 10	Cross-Section 11
1	Removed Even	R801,30	R91,27	R101,32	R111, 25
2	Removed Odd	R802,30	R92,28	R102,33	R112,25
3	Removed 3 <sup>rd</sup>	R803,40	R93,37	R103,44	R113,34
4	Removed 4 <sup>th</sup>	R804,45	R94,42	R104,50	R114,38
5	Removed 5 <sup>th</sup>	R805,48	R95,44	R105,53	R115,40
6	Removed 6 <sup>th</sup>	NA	NA	NA	NA
7	Removed Bed Points	R806,50	R96,45	R106,56	R116,40
8	Removed Surface Points	R807,50	R97,45	R107,56	R117,40
9	Removed Even Panels - A	R812,33	R911,32	R1017,37	R1117,29
10	Removed Odd Panels - B	R813,29	R912,28	R1018,35	R1118, 27
11	Horizontal Slice 2 <sup>nd</sup>	R20,51	R920,47	R1020,58	R1120,42
12	Horizontal Slice 3 <sup>rd</sup>	R822,52	R921,47	R1021,58	R1121,42
13	Horizontal Slice 4 <sup>th</sup>	R823,52	R922,49	R1022,58	R1122,45
14	Horizontal Slice 5 <sup>th</sup>	R824,52	R923,49	R1023,59	R1123,46
15	Horizontal Slice 6 <sup>th</sup>	R825,54	R924,51	R1024,59	R1124,48
16	Horizontal Slice 7 <sup>th</sup>	R826,56	NA	R1025,63	R1125,49
17	Horizontal Slice 8 <sup>th</sup>	R827,57	NA	R1026,63	NA
18	Removed Even Panels - B	R832,41	R927,40	R1027,45	R1126,37
19	Removed Odd Panels - B	R833,37	R928,36	R1028,43	R1127,35
20	0 m sec @ Bed	R816,37	R916,45	R1016,56	R1116, 50

Column 2 describes the type of analysis; R801 stands for the run number followed by the number of control points in the subset (30).

### 3.4.3.2 SYSTEMATIC REMOVAL OF POINTS - PLAN VIEW

The bed speed (sampled at 0.025 m off the bed), surface and average fluid speeds at each of the 10 panels for cross-sections 7 to 11 were used to examine the errors associated with the plan view. Table 3.6 summarizes the types of analyses used in the plan view. The original data set for each speed type used (bed, surface, average) consisted of 50 points (N=50) - 1 value per panel (10 panels at 5 cross-sections).

**TABLE 3.6 SUMMARY OF SYSTEMATIC REMOVAL OF POINTS - PLAN VIEW**

	Description of Analyses	N
1	Removed every point from cross-sections 8 and 10	30
2	Removed every point from cross-sections 9 and 11	30
3	Removed every odd point from data set	25
4	Removed every even point from data set	25

N is the number of control points used as input for computer programs.

### 3.4.3.3 RANDOM REMOVAL OF POINTS

At cross-section 11, points were randomly selected and then removed from the data set using a C-random number

generator based on Plauger (1992) and Johnsonbaugh & Kalin (1989). The program was used to randomly select point numbers from the data set. The corresponding points were then excluded from the data set; these new, smaller data sets were then used as input the series of computer programs. Cross-section 11 was used because the amount of computer space needed to store the results, and the amount of processing time required to execute the programs, was less than the other cross-sections.

Two types of analyses were performed. In the first, one point, number 35, was randomly selected and then removed from the complete data set thereby decreasing the number of control points from 50 to 49. This subset was then used as the input for the interpolating programs. Next, a second point was randomly selected in addition to the originally removed point. This subset of 48 points, with points 35 and 10 missing, was then used as input. This process of randomly selecting one more point was continued until the number of control points (N) was decreased from 49 to 20.

In the second analysis, one point, number 28, was randomly selected and removed creating the smaller, input subset. Next, the data set was reduced to 44 points by randomly selecting 5 more points in addition to point number 28. Two runs with the data set of 44 were completed. In the second run, 5 more points were selected and removed. This dual set of runs with point 28 as the constant was completed



for subsets of 44, 39, and 24 points. As the selection of points was random, it was possible that the same point number could be removed for each dual set of analyses.

The objective of the random analyses was to determine the influence that the number of points has on the interpolant, and the role that point location in space has on the interpolated values.

#### **3.4.4 EXECUTION OF PROGRAMS**

When the number of control points was reduced by either the systematic or random methods to create the smaller, input subset, the programs `matrx1.c` and `svbksb.c` had to be modified. The value for NP and MP in `svbksb.c` and the N in `matrx1.c` had to equal the number of control points.

In the program `xyzpart.c`, 3 changes were necessary. First, the value of N had to equal the number of control points in the input data files (same change as noted above). Secondly, for the cross-section analyses new X and Y coordinates were generated by decrementing by 0.01 m in the X direction and 0.001 m in the Y direction. The values of X and Y were decreased to the point of the width of the distance between panels 1 and 10 (X) and the maximum depth of the cross-section (Y). Thirdly, for each new cross-section, the values for the width and depth needed to be changed.

For the plan view, X and Y were changed to reflect the size of the grid. The length (X) equalled 40, while Y, the width, equalled 32. New points were generated by incrementing by 0.01 cm in both the X and Y directions

The output from xyzpart.c for the cross-section analyses was a file containing XYZ data for points every 0.01 m across the channel and 0.001 below the surface. Due to variations in the width and depth of the 4 cross-sections, the number of points in the file ranged from 249,375 points at CS 11 (width = 6.65m and depth = 0.375 m) to 216,110 points at cross-section 10 (width = 7.71 m and depth = 0.410 m). In the plan view analyses, the number of points generated was 128,721. This value did not change as the size of the grid (40 X 32), and the values used to increment the X and Y coordinates, were constant.

In order to determine the absolute and relative errors of the interpolated points, the original x,y coordinates and the corresponding z value had to be located. To do this, a series of AWK commands (Aho *et al.*, 1988) were written and placed in an AWK file (Table 3.7a).

The entire output from xyzpart.c (ie. 249,375 - 316,110 and 128,721) could not be plotted because of the limitations of the number of pixels on the monitor and because the plotting program, xyzplot.c, plotted values within a certain window. The number of pixels is limited to the type and size of monitor used. The size and scaling of this window were

defined by the user, but due to the size of this window, and the pixel limitation, the complete set of points could not be plotted. In order to plot the interpolated fluid speeds, the number of points in the output file needed to be reduced. This could be done by either writing a series of AWK commands or C routines to extract every 2<sup>nd</sup>, 3<sup>rd</sup>, 4<sup>th</sup> etc point, or xyzpart.c could be rerun with different values used to decrement X and Y. For this study, method 2 was used because of ease of implementation and speed of computing.

In order to determine the points which belonged to each colour class in xyzplot.c, the maximum fluid speed was needed. Again, a series of AWK commands were used to search the input file and print off the maximum speed.

**TABLE 3.7A AWK COMMANDS USED TO LOCATE POINTS**

```

$2~/-0.37/ && $3~/-0.030/ {print $0}
$2~/-0.37/ && $3~/-0.055/ {print $0}
$2~/-1.11/ && $3~/-0.010/ {print $0}
$2~/-1.11/ && $3~/-0.060/ {print $0}
$2~/-1.11/ && $3~/-0.110/ {print $0}
$2~/-1.11/ && $3~/-0.135/ {print $0}
$2~/-1.85/ && $3~/-0.030/ {print $0}
$2~/-1.85/ && $3~/-0.080/ {print $0}
$2~/-1.85/ && $3~/-0.130/ {print $0}
$2~/-1.85/ && $3~/-0.155/ {print $0}

```

For this series of awk commands, \$2 and \$3 are the columns of data representing the X and Y coordinates. These XY coordinates were the original coordinates of the sampled data. In awk, \$0 represents the entire line or row of characters (data). Thus, the first line in table 3.7a reads: find the line of data that has an X coordinate of -0.37 m (note: the data file does not contain units) and a Y coordinate of -0.030 m and print out the entire row of data. This row of data is in the form: X coordinate (m), Y coordinate (m) and Z value (m/s). In this particular example, the series of awk commands will locate the XY coordinates for points in panels 1 to 3 at cross-section 11 in the cross-section analyses.

**TABLE 3.7B AWK COMMANDS USED TO BREAK DATA INTO BLOCKS**

```
awk "NR==1,NR==160000 {print $0}" xyz >>11axyz
awk "NR==16001,NR==32000 {print $0}" xyz >>11bxyz
awk "NR==32001,NR==48000 {print $0}" xyz >>11cxyz
awk "NR==48001,NR==64000 {print $0}" xyz >>11dxyz
```

From the data file xyz (output from xyzpart.c), print all lines (ie. the X,Y and Z values) between 1 and 16,000 inclusive to the output file 11axyz. The limit of 16,000 is a function of the software used to plot the data.

In xyzplot.c the value of N, in this case the number of points to plotted, had a maximum value of 16,000. This meant that no input file could have more than 16,000 points. As most of the files contained more than 16,000 points, the files needed to be broken down into smaller files, each containing 16,000 or less points. This was accomplished by a series of AWK commands (table 3 7b). The xyzplot.c program has a flood fill function which allows the user to colour in any areas below the bed (cross-section) and outside the channel banks (plan view). In order to do this, the X and Y coordinates of various points along the bed and channel needed to be entered into the program. For this thesis, 10 points were selected to outline the bed (the 10 points corresponded to the depth of the panels) for the cross-section analyses and 36 points were selected to delineate the banks of the river.

The general set of commands in the batch file, then, to run the programs and plot the results were:

```
qcl/AL matr1.c
qcl/AL xsvbksb.c nrutil.c svdcmp.c svbksb.c pythag.c
matr1 xy.dat z.dat
xsvbksb
```

```

qcl/AL xyzpart.c
xyzpart xy.dat (produces output file xyz.dat)

awk -f find.awk xyz.dat >> foundfile (find.awk -
awk commands used to locate points; foundfile = the
output file contain the XYZ data)

awk -f largest.awk xyz.dat (largest.awk - awk
commands used to identify the maximum fluid speed)

awk -f break.awk xyz.dat (awk routines used to
create files of 16,000 points)

qcl/AL xyzplot.c
xyzplot file1 file2 file3 (file 1,2,3 are blocks of
16,000)

```

### 3.4.5 CALCULATION AND GRAPHING OF ERRORS

To achieve the objective of quantify the errors associated with the method, the absolute and relative errors were calculated using the following equations:

$$(12) \quad AE = Z_k - Z_1$$

and

$$(13) \quad RE = ((Z_k - Z_1) / Z_k) * 100,$$

where AE is the absolute error in m/sec, RE is the relative error expressed as percent,  $Z_k$  is the known fluid speed, and  $Z_1$  is the interpolated fluid speed. Equation 12 is similar to the PDVEL statistic used by Bray (1979) to evaluate the effectiveness of various equations used to predict fluid speeds at points in a vertical.

The magnitude of the errors was examined by plotting histograms for both the relative and absolute errors. For the relative error, the class interval used was 10%, while the

class interval for the absolute error was 0.05 m/s. For both the cross-section and plan view analyses 20 classes were used ranging from greater than -100% to greater than 100%. The class range used for the absolute error in the cross-section analyses was -0.65 m/s to 0.60 m/s, while for the plan view analyses, it was -0.85 m/s to 0.60 m/s.

To examine the spatial distribution of errors, the histograms for both types of analyses were compared against each other. In the cross-section analyses, the maximum distance between nearest neighbours in a vertical was 0.05 m. The distance between adjacent panels at a cross-section ranged from tens of centimetres to a few metres. The distance between adjacent points at a cross-section in plan view was the same as the distance between adjacent panels in the cross-section analyses, while the distance between cross-sections was on the order of several metres.

The spatial distribution of errors in the cross-section analyses was further analyzed by looking at the magnitude of the errors as a function of the position both within a vertical and across the channel.

## CHAPTER 4: RESULTS

### 4.1 SYSTEMATIC REMOVAL OF POINTS: CROSS-SECTION ANALYSES

In total, cross-sections 8 and 10 had 17 systematic analyses, cross-section 9 had 15 and cross-section 11 had 16 (table 3.5). In addition, 30 random analyses were done on cross-section 11.

Table 4.1 summarizes the results for the systematic removal of points (row 1-8 and 11-17 table 3.5) for cross-section 11. Columns 1 and 2 are the X and Y coordinates for each known speed, column 3. "Max/min int", column 4, are the maximum and minimum interpolated values for each point from the different analyses. Column 5 has the maximum and minimum absolute error for each point. The difference between interpolated points from the different runs in meters/sec is in column 6. The maximum and minimum relative error for each point is column 7. The last column, labelled N, is the number of control points used in the interpolated routines for the different systematic removal analyses. The results for runs R1117/1118 and R1126/1127, the panel removal runs (row 8,9 and 17,18 in table 3.5) are in table 4.2. If there was no difference between the different analyses (a 0 in column 6), then only one value will be listed in columns 4 and 5.

TABLE 4.1 SUMMARY OF ABSOLUTE AND RELATIVE ERRORS - CROSS-SECTION 11

X	Y	Z (m s)	Max, Min Int. (m. s)	Max Min ΔE(m s)	Diff Int	Max Min RE (%)	N
-0.37	-0.030	0.303	0.298, 0.300	-0.003, -0.005	0.002	1.00, 1.65	25, 40
-0.37	-0.055	0.285	0.300, 0.302	-0.015, -0.017	0.002	-5.26, -5.97	25, 40, 40
-1.11	-0.010	0.544	0.590, 0.601	-0.046, -0.054	0.011	-8.46, -10.48	25, 34, 40, 40
-1.11	-0.060	0.588	0.498	0.090	0.000	15.31	25, 38, 42
-1.11	-0.110	0.453	0.450	0.003	0.000	0.066	25, 40, 42
-1.11	-0.135	0.381	0.435, 0.444	-0.054, -0.063	0.009	-14.17, -16.54	25, 34, 40, 40
-1.85	-0.030	0.567	0.533, 0.547	0.020, 0.034	0.014	3.53, 6.00	25, 40, 40
-1.85	-0.080	0.512	0.490	0.022	0.000	4.30	25, 38, 42
-1.85	-0.130	0.413	0.329	0.084	0.000	20.34	25, 34, 42
-1.85	-0.155	0.237	0.348, 0.407	-0.161, -0.170	0.009	-67.93, -71.73	25, 40, 40, 40
-2.59	-0.030	0.662	0.618, 0.633	0.029, 0.044	0.015	4.38, 6.65	25, 40, 40
-2.59	-0.080	0.601	0.561, 0.562	0.039, 0.040	0.001	6.49, 6.66	25, 34, 38, 42
-2.59	-0.130	0.461	0.371	0.090	0.000	19.52	25, 42
-2.59	-0.155	0.256	0.446, 0.453	-0.190, -0.197	0.007	-74.22, -76.95	25, 40, 40
-3.33	-0.005	0.487	0.665, 0.681	-0.178, -0.194	0.016	36.55, 39.43	25, 34, 40, 40, 40
-3.33	-0.055	0.648	0.518	0.130	0.000	20.06	25, 38, 42
-3.33	-0.105	0.548	0.594, 0.595	-0.046, -0.047	0.001	-8.39, -8.58	25, 42
-3.33	-0.155	0.541	0.371	0.170	0.000	31.42	25, 34, 45
-3.33	-0.180	0.282	0.520, 0.528	-0.238, -0.246	0.008	-84.40, -87.23	25, 40, 40
-4.07	-0.005	0.549	0.631, 0.644	-0.082, -0.095	0.013	-14.94, -17.03	25, 38, 40, 40, 40
-4.07	-0.055	0.605	0.533	0.072	0.000	11.90	25, 34, 42
-4.07	-0.105	0.516	0.512	0.004	0.000	0.078	25, 42
-4.07	-0.155	0.419	0.404, 0.405	0.014, 0.015	0.001	3.34, 3.58	25, 45
-4.07	-0.205	0.292	0.266	0.026	0.000	8.90	25, 34, 38, 45
-4.07	-0.230	0.189	0.271, 0.284	-0.082, -0.095	0.013	-43.39, -50.26	25, 40, 40, 40
-4.81	-0.020	0.579	0.641, 0.654	-0.062, -0.070	0.013	-10.71, -12.95	25, 40, 40, 40
-4.81	-0.070	0.621	0.585	0.036	0.000	5.80	25, 34, 42
-4.81	-0.120	0.590	0.544	0.046	0.000	7.80	25, 38, 42
-4.81	-0.170	0.467	0.444	0.023	0.000	4.93	25, 45
-4.81	-0.220	0.298	0.209	0.089	0.000	29.87	25, 34, 40, 46
-4.81	-0.245	0.080	0.281, 284	-0.201, -0.204	0.003	-251.25, -255.00	25, 40, 40
-5.55	-0.350	0.537	0.548, 0.557	-0.011, -0.020	0.009	-2.05, -3.72	25, 38, 40, 40



-5.55	-0.085	0.523	0.468	0.055	0.000	10.52	25,34,42
-5.55	-0.135	0.398	0.416	-0.018	0.000	-4.53	25,42
-5.55	-0.185	0.309	0.345	-0.036	0.000	-11.65	25,40,45
-5.55	-0.235	0.291	0.191	0.100	0.000	34.36	25,34,38,46
-5.55	-0.285	0.072	0.126	-0.054	0.000	-75.00	25,48
-5.55	-0.310	0.043	0.066,0.067	-0.023,-0.024	0.001	-53.49,-55.81	25,40,40
-6.28	-0.025	0.490	0.482,0.493	0.008,-0.003	0.011	1.63,-0.061	25,34,40,40
-6.28	-0.75	0.473	0.479	-0.006	0.000	-1.27	25,38,40,42
-6.28	-0.125	0.464	0.429	0.035	0.000	7.54	25,42
-6.28	-0.175	0.385	0.379	0.006	0.000	1.56	25,34,45
-6.28	-0.225	0.295	0.316	-0.021	0.000	-7.12	25,46
-6.28	-0.275	0.249	0.266	-0.017	0.000	6.83	25,38,48
-6.28	-0.325	0.238	0.137	0.101	0.000	42.43	25,34,40,49
-6.28	-0.350	0.081	0.218,0.221	-0.137,-0.140	0.003	-169.14,-172.84	25,40,40
-7.02	-0.040	0.218	0.04,0.0493	0.175,0.169	0.006	80.28,77.52	25,40,40
-7.02	-0.090	0.013	0.109	-0.096	0.000	-738.46	25,34,38
-7.02	-0.140	-0.001	0.012	-0.013	0.000	1300	25
-7.02	-0.165	0.011	-0.002,-0.007	0.013,0.004	0.005	118.18,36.36	25,40,40,40

Refer to text for explanation of table

**TABLE 4.2 SUMMARY OF ABSOLUTE AND RELATIVE ERROR - PANEL REMOVAL RUNS - CROSS-SECTION 11**

X	Y	Z (m/s)	R1117/R1118 Int (m/s)	Absolute Error (m/s)	Relative Error (%)	R1127/R1128 Int (m/s)	Absolute Error (m/s)	Relative Error (%)
-0.37	-0.030	0.303						
-0.37	-0.055	0.285						
-1.11	-0.010	0.544	0.375	0.169	31.07			
-1.11	-0.060	0.588	0.357	0.231	39.29	0.478	0.110	18.71
-1.11	-0.110	0.453	0.340	0.113	29.94	0.413	0.040	8.83
-1.11	-0.135	0.381	0.331	0.050	13.12			
-1.85	-0.030	0.567	0.499	0.068	11.99			
-1.85	-0.80	0.512	0.475	0.037	7.23	0.436	0.076	14.84
-1.85	-0.130	0.413	0.451	-0.038	-9.20	0.303	0.110	26.63
-1.85	-0.155	0.237	0.438	-0.201	-84.81			
-2.59	-0.030	0.662	0.440	0.222	33.53			
-2.59	-0.080	0.601	0.417	0.184	30.62	0.500	0.101	16.81
-2.59	-0.130	0.461	0.394	0.067	14.53	0.337	0.124	26.90
-2.59	-0.155	0.256	0.382	-0.126	-49.22			
-3.33	-0.005	0.487	0.487	0.000	0.00			
-3.33	-0.055	0.648	0.458	0.190	29.32	0.429	0.219	33.80
-3.33	-0.105	0.548	0.429	0.119	21.72	0.371	0.277	32.30
-3.33	-0.155	0.541	0.399	0.149	26.75	0.312	0.229	42.33
-3.33	-0.180	0.282	0.384	-0.102	-36.17			
-4.07	0.005	0.549	0.448	0.101	18.40			
-4.07	0.055	0.605	0.422	0.183	30.25	0.470	0.135	22.31
-4.07	0.105	0.516	0.394	0.122	23.64	0.391	0.125	24.22
-4.07	0.155	0.419	0.366	0.053	12.65	0.310	0.109	26.01
-4.07	0.205	0.292	0.338	-0.046	-15.75	0.230	0.062	21.23
-4.07	0.230	0.189	0.323	-0.134	-70.90			
-4.81	0.020	0.579	0.426	0.153	26.42			
-4.81	0.070	0.621	0.396	0.225	36.23	0.469	0.152	24.48
-4.81	0.120	0.590	0.366	0.224	37.97	0.359	0.231	39.15
-4.81	0.170	0.467	0.335	0.132	25.27	0.247	0.220	47.11
-4.81	0.220	0.298	0.304	-0.006	-2.01	0.136	0.162	54.36
-4.81	0.245	0.080	0.288	-0.208	-260.00			
-5.55	0.035	0.537	0.422	0.115	21.42			
-5.55	0.085	0.523	0.393	0.130	24.86	0.449	0.074	14.15
-5.55	0.135	0.398	0.363	0.035	8.79	0.361	0.037	9.30
-5.55	0.185	0.309	0.331	-0.022	-7.12	0.271	0.038	12.30
-5.55	0.235	0.291	0.300	-0.009	-3.09	0.180	0.111	38.14
-5.55	0.285	0.072	0.268	-0.196	-272.22	0.089	-0.017	-23.61
-5.55	0.310	0.043	0.252	-0.209	-486.05			
-6.28	0.025	0.490	0.268	0.222	45.31			
-6.28	0.075	0.473	0.242	0.231	48.84	0.425	0.048	10.15
-6.28	0.125	0.464	0.216	0.248	53.45	0.361	0.103	22.20
-6.28	0.175	0.385	0.190	0.195	50.65	0.297	0.088	22.86
-6.28	0.225	0.295	0.164	0.131	44.41	0.234	0.061	20.68
-6.28	0.275	0.249	0.138	0.111	44.58	0.172	0.077	30.92
-6.28	0.325	0.238	0.113	0.125	52.52	0.111	0.127	53.36
-6.28	0.350	0.081	0.101	-0.020	-24.69			
-7.02	0.040	0.218						
-7.02	0.090	0.013						
-7.02	0.140	-0.001						
-7.02	0.165	0.011						

Table 4.3 summarizes the variation in interpolated values

for each point in the systematic removal of single point values (rows 1-8, 11-17, table 3.5). Column 2 is the total number of points in each cross-section. Column 3 is the number of points in each section that showed no variation in interpolated values between the different runs. Column 4 gives the number of bed and surface points that showed variation in the interpolated values (note: for each cross-section the maximum number of bed/surface points is 20, except at number 8, where the number is 18). Columns 5 through 8 indicate the number of points for each cross-section that had differences in interpolated values ranging from 0.001 m/s to greater than 0.010 m/s. The last column gives the maximum difference between interpolated points.

For example, at cross-section 8 the near surface point (-0.005m below the surface) at panel 3 was removed in 3 analyses (R802, R805, R807 - table 3.5). The interpolated values for those analyses were 0.003 m/s, 0.002 m/s and 0.005 m/s. The range, then, is 0.003 m/s. The point at 0.055 m below the surface (1 point below the near surface point) was also removed in 3 analyses (R801, R803, R820). The interpolated value for all 3 analyses was 0.005 m/s; the variation is 0.000 m/s.

For analyses in which even and odd panels were removed (table 3.5), no point had the same interpolated values between runs a and b.

**TABLE 4.3 DIFFERENCES IN INTERPOLATED VALUES**

Cross-Section Number	Number of points in Cross-section	Number of points with no variation	Number at Bed or Surface that had variations	0.001 m/s	0.002-0.005 m/s	0.006-0.010 m/s	>0.010 m/s	Max. Variation m/s
8	59	34	17	9	7	7	2	0.011
9	55	258	20	9	11	7	0	0.009
10	66	40	20	8	17	1	0	0.006
11	50	27	20	4	5	6	8	0.016

Column 3 indicates perfect agreement for single points in the different runs. Column 4 indicates how many of the points on the convex shell had perfect agreement. The remaining columns show the range in values of the interpolated points across the different analyses.

An absolute error of 0 m/s and a relative error of 0 % indicates that the interpolated fluid speed was the same as the known speed. The following table, table 4.4, summarizes the location of the points, and the analyses (column 4) at which the 0 values happened.

**TABLE 4.4 LOCATION AND ANALYSES WITH ERROR VALUES OF 0**

Cross-Section #	X Coord (m)	Y Coord (m)	Run(s)
8	-3.40	-0.110	R801, R821
8	-2.64	-0.115	R812
8	-1.89	-0.205	R833
9	-3.38	-0.005	R97
10	-2.14	-0.080	R102, R103, R1020
10	-6.43	-0.005	R104
10	-6.43	-0.225	R1017
11	-3.33	-0.005	R1118

The average absolute and relative errors for cross-sections 8-11 are presented in table 4.5 to table 4.8 for the

analyses in which the even/odd number points were removed as well as for both sets on analyses in which all the points in a panel were removed. The average values are based on the combined values for each analysis; the average value of -0.003 m/s for R81/82 was based on 60 points - 30 for R81 and 30 for R82. The averages denoted by the asterisks (\*) were based on the absolute values for each point.

**TABLE 4.5 SUMMARY OF ABSOLUTE AND RELATIVE ERRORS - CROSS-SECTION 8**

	R81/82 <sup>1</sup>		R812/813 <sup>2</sup>		R832, 833 <sup>3</sup>	
	AE (m/s)	RE (%)	AE (m/s)	RE (%)	AE (m/s)	RE (%)
Avg.	-0.003	-54.62	0.092	19.05	0.130	57.41
Avg.*	0.044	109.25	0.158	172.84	0.133	64.32
Avg. no boundary	0.020	27.30	0.120	130.68	NA	NA
Avg. no boundary*	0.037	42.58	0.158	141.46	NA	NA
Avg. Bed	-0.093	-462.37	-0.058	-333.60	NA	NA
Avg. Bed*	0.100	474.41	0.135	357.48	NA	NA
Avg. Surface	-0.030	-10.98	0.107	-56.65	NA	NA
Avg. Surface*	0.032	34.99	0.182	135.23	NA	NA

\* Average based on the absolute values of absolute and relative errors.

1 - Column 2 (tables 4.5 to 4.8): SVR Run

2 - Column 3 (tables 4.5 to 4.8): Panel Removal Run - removed all points in a panel

3 - Column 4 (tables 4.5 to 4.8): Panel Removal Run Boundary - kept near bed and surface points

**TABLE 4.6 SUMMARY OF ABSOLUTE AND RELATIVE ERRORS - CROSS-SECTION 9**

	R91/92		R912/913		R932/933	
	AE (m/s)	RE (%)	AE (m/s)	RE (%)	AE (m/s)	RE (%)
Avg.	-0.003	-4.45	0.066	77.99	0.102	37.18
Avg.*	0.047	39.95	0.130	109.74	0.116	42.62
Avg. no boundary	0.018	4.12	0.087	44.58	NA	NA
Avg. no boundary*	0.042	24.50	0.131	70.50	NA	NA
Avg. Bed	-0.070	-39.93	-0.110	-273.82	NA	NA
Avg. Bed*	0.085	-107.74	0.110	362.12	NA	NA

Avg. Surface	-0.011	0.028	0.112	24.10	NA	NA
Avg Surface*	1.83	11.78	NA*	NA*	NA	NA

\* Average based on the absolute values of absolute and relative errors  
 \* All values were positive

**TABLE 4.7 SUMMARY OF ABSOLUTE AND RELATIVE ERRORS -  
 CROSS-SECTION 10**

	R101/102		R1017/1018		R1027/1028	
	AE (m/s)	RE (%)	AE (m/s)	RE (%)	AE (m/s)	RE (%)
Avg	-0.003	-19.26	0.040	14.35	0.068	30.63
Avg.*	0.029	36.69	0.070	49.50	NA*	NA*
Avg. no boundary	0.013	5.52	0.057	-14.08	NA	NA
Avg. no boundary*	0.018	9.70	0.063	30.02	NA	NA
Avg. Bed	-0.055	-145.54	-0.182	9.10	NA	NA
Avg Bed*	0.056	193.60	0.189	158.21	NA	NA
Avg Surface	-0.023	-7.79	0.062	21.05	NA	NA
Avg Surface*	0.025	9.35	NA*	NA*	NA	NA

\* Average based on the absolute values of absolute and relative errors  
 \* All values were positive

**TABLE 4.8 SUMMARY OF ABSOLUTE AND RELATIVE ERRORS -  
 CROSS-SECTION 11**

	R111/112		R1117/1118		R1127/1128	
	AE (m/s)	RE (%)	AE (m/s)	RE (%)	AE (m/s)	RE (%)
Avg	-0.007	2.11	0.068	-9.75	0.113	26.35
Avg.*	0.067	70.25	0.128	50.31	0.113	26.35
Avg. no boundary	0.031	24.56	0.108	13.63	NA	NA
Avg. no boundary*	0.052	81.42	0.128	35.73	NA	NA
Avg Bed	-0.111	-64.62	-0.119	-123.78	NA	NA
Avg Bed*	0.114	90.07	-0.130	129.78	NA	NA
Avg Surface	-0.016	1.50	0.131	23.77	NA	NA
Avg Surface*	0.065	16.95	0.131	23.77	NA	NA

\* Average based on the absolute values of absolute and relative errors

The absolute and relative error frequency diagrams for the analyses from tables 4.5 to 4.8 are displayed in figures 4.1 to 4.4.

#### **4.2 RESULTS: RANDOM REMOVAL OF POINTS**

Point 35 was removed from the input file when the size of the file varied from 49 to 20 (ie.  $N = 49$ ,  $N=20$ ). The interpolated value was 0.345 m/s when  $N=49$  to  $N=27$  and it was 0.344 m/s when  $N$  decreased from 27 to 20. The difference, then, was 0.001 m/s across the analyses. It should be pointed out that in all these analyses no adjacent points in the vertical were removed. Two other points were also removed without adjacent points being removed. Point number 1, panel 1 was removed from the analysis in which the input data set decreased from 43 to 20; the interpolated value ranged from 0.298 m/s to 0.294 m/s, a difference of 0.004 m/s. Point 3, at the top of panel 3 was removed in 22 analyses ( $N$  decreased from 41 to 20). The interpolated values ranged from 0.597 m/s to 0.585 m/s, a range of 0.012 m/s.

FIGURE 4.1A ABSOLUTE ERROR - CS 8

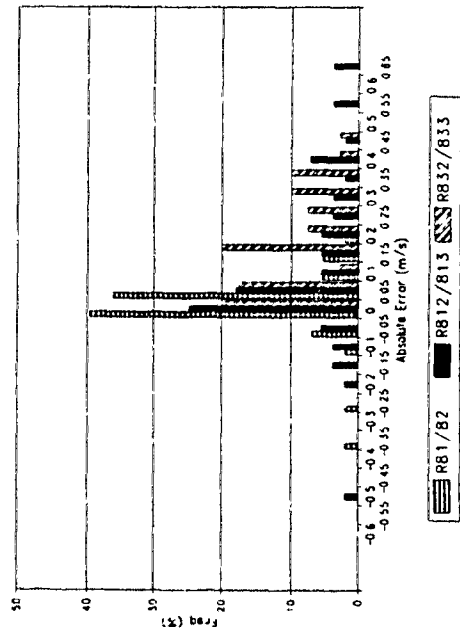
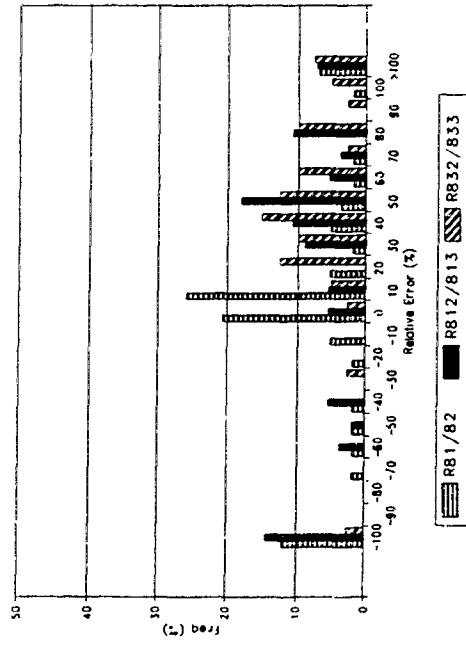


FIGURE 4.1B RELATIVE ERROR - CS 8





FIGURES 4.2A ABSOLUTE ERROR - CS 9

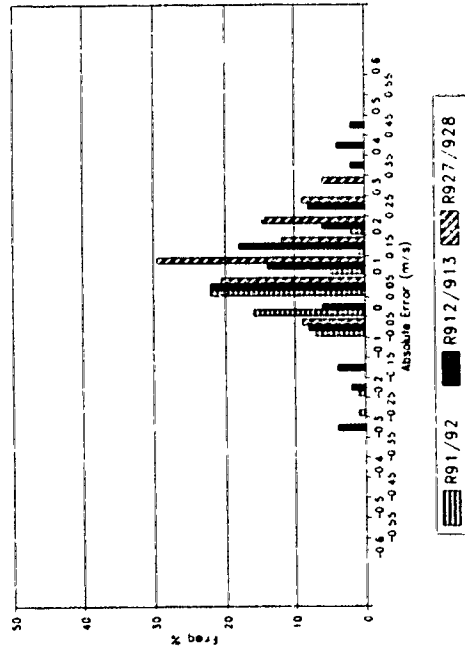


FIGURE 4.2B RELATIVE ERROR - CS 9

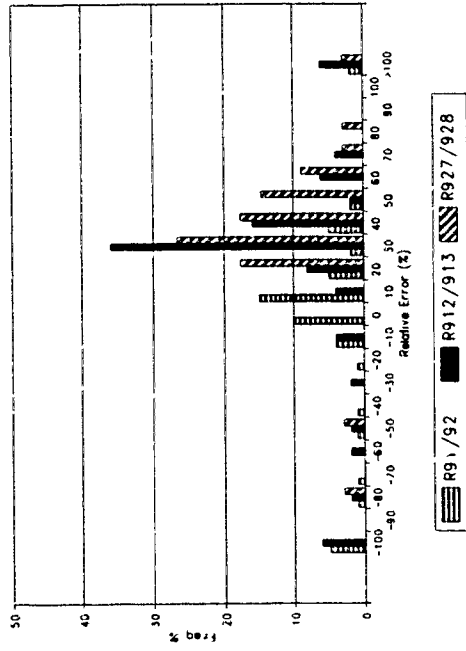


FIGURE 4.3A ABSOLUTE ERROR - CS 10

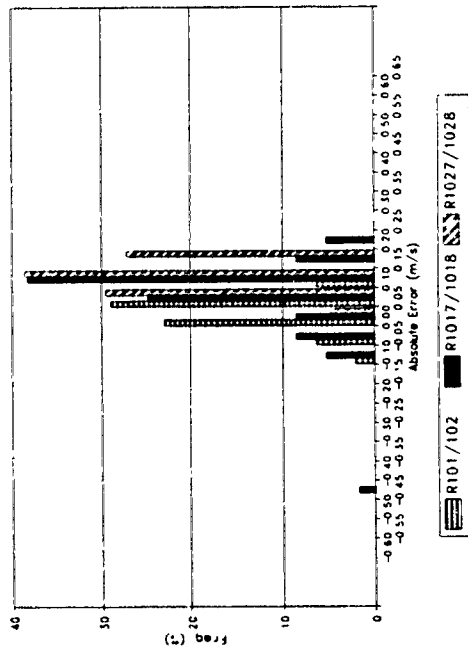


FIGURE 4.3B RELATIVE ERROR - CS 10

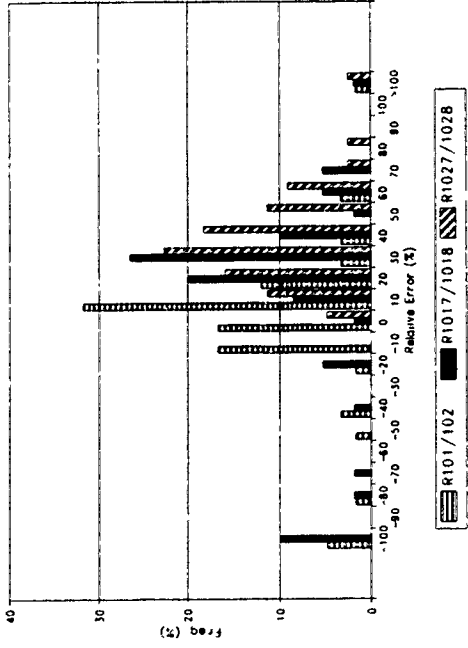


FIGURE 4.4A ABSOLUTE ERROR - CS 11

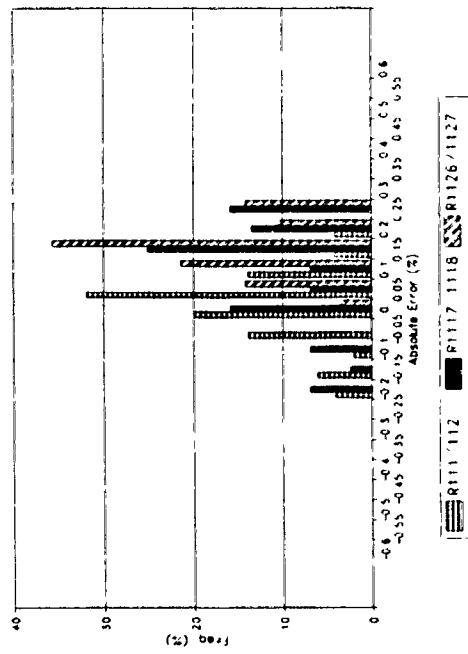
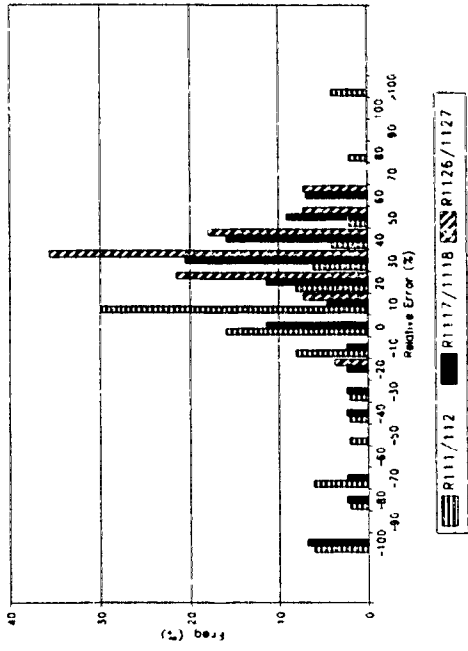


FIGURE 4.4B RELATIVE ERROR - CS 11



For the points that were removed in a vertical in which adjacent points were also removed, a pattern in the value of interpolants appears. As long as no points immediately above or below are removed, there is little variation in the interpolated value. When an adjacent point was removed, the value changed. At panel 9, point 42 was removed when  $N=47$ ; the interpolated value was 0.377 m/s. This value remained the same until  $N$  decreased to 29, when point 41 was removed. Point 40, also at panel 9, had an interpolated value of 0.477 m/s when  $N$  ranged from 39 to 29 (i.e. when point 41 was removed). The values interpolated for points 40, 41, and 42, when  $N$  decreased from 29 to 27 was 0.440 m/s, 0.391 m/s and 0.343 m/s. When the point 39 was removed, the near surface point in this panel, the interpolated values for points 40 to 42 changed.

When point 28 was removed in the second type of random analyses (recall in the second type of random analyses, the data set was reduced in size from 44, to 39 to 24, with point 28 being a constant in all sets of data), the interpolated value was 0.544 m/s. For the pair of analyses when  $N=44$ , the interpolated value was 0.544 m/s and 0.514 m/s. In the later case, the point below was removed (pt. 29, interpolated value = 0.406 m/s). In the runs in which  $N=39$ , the interpolated value for point 28 was 0.505 m/s and 0.544 m/s. In the first case the point immediately above it was removed (interpolated

value for point 27 was 0.542 m/s). In the last pairing of analyses, when N=24, the interpolated values for point 28 were 0.514 m/s and 0.366 m/s. In the first analysis when N=24, point 29 was removed and the interpolated value for this point was 0.406 m/s (the values for points 28 and 29 in this analysis are the same as those when N = 44). In the second analysis when N=24, both the point above and below were removed (table 4.9)

**TABLE 4.9 INTERPOLATED VALUES FOR PANEL 7 - RANDOM ANALYSES**

Point #	N=49	N=44	N=44	N=39	N=39	N=24	N=24
26							
27				0.542			0.399
28	0.544	0.544	0.514	0.505	0.544	0.514	0.366
29			0.406			0.406	0.406
30				0.209			
31							

In this analyses, point 28 was removed from all runs as N decreased from 49 to 24. Other points were randomly removed from the data set. This table shows the interpolated values for points in panel 7 in these different runs. Note how the value interpolated for point 28 changes as the nearest neighbour(s) are removed and interpolated.

The values interpolated when single points were removed in the random analyses were comparable in range to those in the systematic removal of points. In many cases, the same

value was interpolated. As a result, the absolute and relative errors between the two types of analyses did not change. There was little variation in the range of interpolated values at a point between the systematic removal of points and the two types of random removal.

### **4.3 ANALYSIS AND INTERPRETATION**

#### **4.3.1 INTRODUCTION**

A negative absolute error in figures 4.1 to 4.4 and tables 4.5 to 4.8 indicates that the interpolated speeds were greater than the known speeds; in other words, the interpolated values were over-estimates. From tables 4.5 to 4.8 it can be seen that the average absolute error for runs R81/82, R91/92, R101/102 and R111/112 are negative. The largest average value is -0.007 m/s at panel 11. The largest absolute error for this set of runs is -0.379 m/s at the near-bed point of panel 8 and CS8. For all four cross-sections, in this set of runs, near-bed velocities were over-estimated 32 out of 39 times - 6/9 at CS8, 8/10 at CS9, and 9/10 at both CS10 and CS11; while near surface velocities were over-estimated 23 of 39 times - 7/9 at CS8, 6/10 at CS9 and CS10 and 4/10 at CS11.

To eliminate the effect of negative and positive errors

cancelling each other out, the absolute value for each point was used to calculate both the absolute and relative errors (indicated by an \* in tables 4.5 to 4.8). Cross-section 11 again had the largest average absolute error, 0.067 m/s, followed by CS9, CS8 and CS10.

Cross-section 8 had the largest average relative error, based on both the absolute and true values, while CS11 had smallest average based on the true values (table 4.5 to 4.8). The greatest single relative error is -1647.83 % located at the near bed point of panel 8, CS8. Cross-section 8 had 2 relative errors greater than 1000% and 10 between |100.00 and 999.00%| (Figure 4.1a); CS9 had 7 between |100.00 and 999.00 %| (Figure 4.2a); CS10 had 4 between |100.00-999.00%| (Figure 4.3a) and CS11 had 4 between |100.00 % and 999.00%| and 1 over 1000.00%, 1300.00 % at panel 10, 0.025 m above the bed (Figure 4.4a).

#### **4.3.2 GEOGRAPHIC DISTRIBUTION OF ERROR - CROSS-SECTION ANALYSES**

In general, the largest absolute and relative errors at all four cross-sections occur in the boundary and near-boundary areas. The boundary points are those points that are on the convex shell of the data set. The boundary area consists of the near-bed points, 0.025 m above the bed, points at 0.050 m above the bed and near-surface points. At CS8 the

two largest absolute errors,  $-0.379$  m/s and  $0.265$  m/s are at the near-bed points of panels 8 and 7 followed by the points at  $0.05$  m above the bed also at panels 8 and 7; the largest relative errors for this section are at the beds of panels 8, 10 and 3. For CS9, the four largest absolute errors are at the near-bed (two largest) and  $0.05$  m above the bed at panels 8 and 7. The largest relative errors are at the near-bed points of panels 8, 7 and 9 followed by the point at  $0.050$  m above the bed at panel 6. Four of the five largest absolute errors are at the near-bed points of panels 5, 7, 8 and 4 at CS11. The first is the near-surface point at panel 5. The largest relative error for this CS,  $1300.00\%$  is at the points  $0.050$  m above the bed at panel 10, followed by  $-738.46\%$  at a point  $0.150$  m above the bed (2 points below the surface) at panel 10. The relative errors at the beds of panels 7, 9 and 10,  $-251.25\%$ ,  $-169.14\%$  and  $127.27\%$  respectively, make up the remaining five largest errors.

When the boundary points are removed - near-bed and near-surface, the relative errors for runs R81/82, R91/92 and R101/102 decrease for both the true and absolute values (tables 4.5 to 4.7). At CS11, the values increase because the largest error,  $1300.00\%$  is at a point  $0.050$  m above the bed and therefore included in the no boundary average. The relative error of  $2.11\%$  is also influenced by this extreme value. The value is influencing the averages. The near-bed



errors, both absolute and relative, are greater than either the near-surface only and the errors based on the averages of all points taken together. Cross-section 8 had the largest relative errors, > 450.00% (table 4.5).

#### **4.3.3 DISTRIBUTION OF ERROR AND NEAREST NEIGHBOUR POINTS**

The smallest absolute and relative errors for the single point removal analyses are for those points at which the known speed is close to the average speed of the points immediately above and below it. For run R82, at a point 0.110 m below the surface at panel 5, the interpolated value was 0.171 m/s, the same value as the sampled speed. The known value at 0.060 m below the surface (immediately above the removed point) was 0.094 m/s, while the speed at 0.160 m below the surface was 0.244 m/s; the average of these two points is 0.171 m/s. Similarly, at CS10, panel 3, 0.080 m below the surface the interpolated value for runs R102, R103 and R1023 was 0.333 m/s, the same as the average of the two nearest neighbours. The location of 0 % relative error, and 0 m/s absolute error is at those points that lie on the straight line between nearest neighbours.

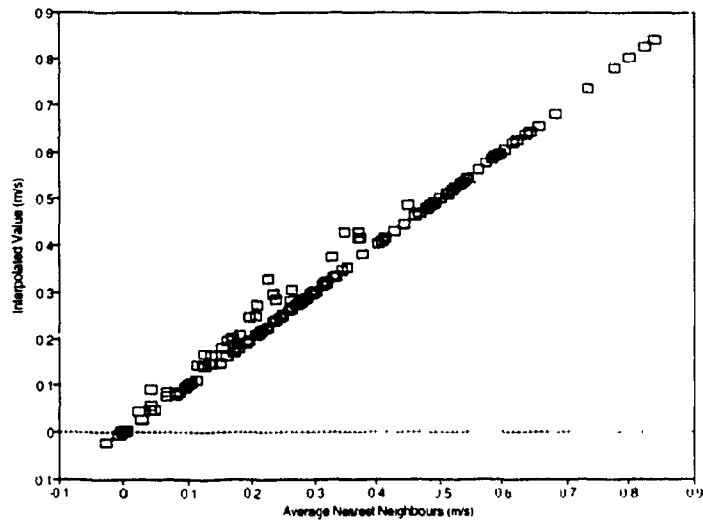
When single points are removed from the data set, the interpolated values are linear; that is, the interpolated value is very close to, if not exactly the same as, the

average of the nearest neighbours. In cases where there is only one nearest point in the profile, the interpolated value is a linear extension of the existing profile. It is for this reason that the near-surface points at panel 5, CS 5, R97 and panel 3 at CS10, R104 have error values of 0 m/s and 0%. Figure 4.5 is a plot of the interpolated values versus the average of the nearest neighbours. The total number of points for the plot is 148, which represents all those acceptable points for analyses R81/82, R91/92, R101/102 and R111/112.

The strong influence of the nearest neighbours is also evident when a point in the profile has a negative number, that is, it is in a region of reverse flow. When a point that is immediately below this negative number is removed, the interpolated value will tend to also be negative. In instances where the point 0.05 m above the bed is negative, but the near bed point (0.025 m above the bed) is positive, the interpolated value for the near bed point will always be negative in the single value removal analyses.

An example of this is at panel 10, CS11. The average speed at 0.05 m above the bed was -0.001 m/s, while the value 0.025 m above the bed was 0.011. The interpolated value was always negative in both the systematic and random removal analyses.

**FIGURE 4.5 AVERAGE NEAREST NEIGHBOUR VS. INTERPOLATED VALUES**



For runs R812/813, R911/912, R1017/1018 and R1117/1118 alternate panels, including the near-bed and surface points were removed. On average, the interpolated values were under-estimates of the known speeds (indicated by a positive sign in tables 4.5 to 4.8). However, similar to the SVR runs, near bed points were overestimated (negative values in table). For runs R812/813, R1017/1018 and R1117/1118 8 out of 8 near bed points were over-estimated, while for runs R911/912, 7 out of 8 were over estimated.

#### 4.3.4 MAGNITUDE OF ERROR - CROSS-SECTION AND PANEL RUNS COMPARED

There is a shift in the magnitude and distribution of errors from the SVR to the panel runs. The average absolute error for all points in the panel removal runs are higher than the corresponding averages for the SVR (AVG and AVG\* in tables 4.5 to 4.8). The relative errors at CS9 and CS10 are both higher in this set of panel analyses. At CS8, R812/813, the average relative error based on the true number values is smaller than the average for runs R81/82 because of the cancelling-out effect of extreme positive and negative values. The relative error based on the absolute values for R111/R112 is higher than R1117/1118 because of the influence of the extreme values at panel 10.

From figures 4.1 to 4.4 the number of absolute errors within +/- 0.009 m/s and the number of relative errors within +/- 10% is smaller for the panel removal runs than for the SVR runs. There is a greater percentage of interpolated values within +/- 0.009 m/s of the known speeds for the single point removal runs (SVR), than there is for the runs in which all the points in a panel were removed (24.8% for the former, and 5.38 % for the latter). This shift to larger error values is also evident in the relative error. The percentage of single value point errors within |5.00 %| is 26.3%, while the percentage for the panel removal runs is 3.8%. For error

values between  $|6.00\% \text{ to } 10.00\%|$ , there are more single value points than panel removal points (22.1% compared to 3.6%). In total, almost 50.0% of the interpolated values in the SVR were within  $\pm 10.00\%$  of the known speeds, while only 9.4% of the panel removal points were within this range.

Cross-section 8 has the largest average absolute error based on both the true and absolute values for this set of analyses (table 4.5). The largest average relative error based on all points is also at CS8. The greatest relative error is -2365.25% at the bed of panel 8 followed by 2300.00% at a point -0.105 m below the surface at panel 3.

For runs R812/813 there are 5 absolute errors greater than 0.500 m/s, four of which are at the top four points in the profile at panel 9. Twenty-one (35.6% of the data) are between 0.100 m/s and 0.499 m/s. There are 2 relative errors greater than 2000.00%, 2 between 500.00% and 900.00% and 8 between 100.00%-499.00% (Figure 4.1a,b). Cross-section 9 has 24 points (48% of the interpolated points) between 0.100 m/s and 0.500 m/s with 2 relative errors greater than 1000% and 4 between 100.00% and 900.00%. There are 11 points between 0.100 and 0.200 m/s at CS10 and 1 relative error over 500.00% with 5 relative errors between 100.00% and 499.00%. At CS11, 11 points were between 0.100-0.200 m/s with 3 relative errors between 100.00% and 500.00% (Figure 4.4a,b)

#### **4.3.5 GEOGRAPHIC DISTRIBUTION OF ERRORS - PANEL RUNS**

The pattern of largest relative error occurring at and near the bed identified for the SVR runs is also visible for the panel removal runs. At CS8, R812/813, 2 of the 5 largest errors are the bed and surface of panels 8 and 5. For CS9, 4 of the 5 largest errors are at the bed and near-bed points of panels 6 and 9, while the fourth largest is at a point 0.010 m above the bed at panel 6. The largest relative errors at CS10 are located at the bed and near-bed point of panel 8, and at the beds of panels 7,3 and 5. The two largest errors at CS11 were located at points 0.025 m and 0.050 m off the bed at panel 8.

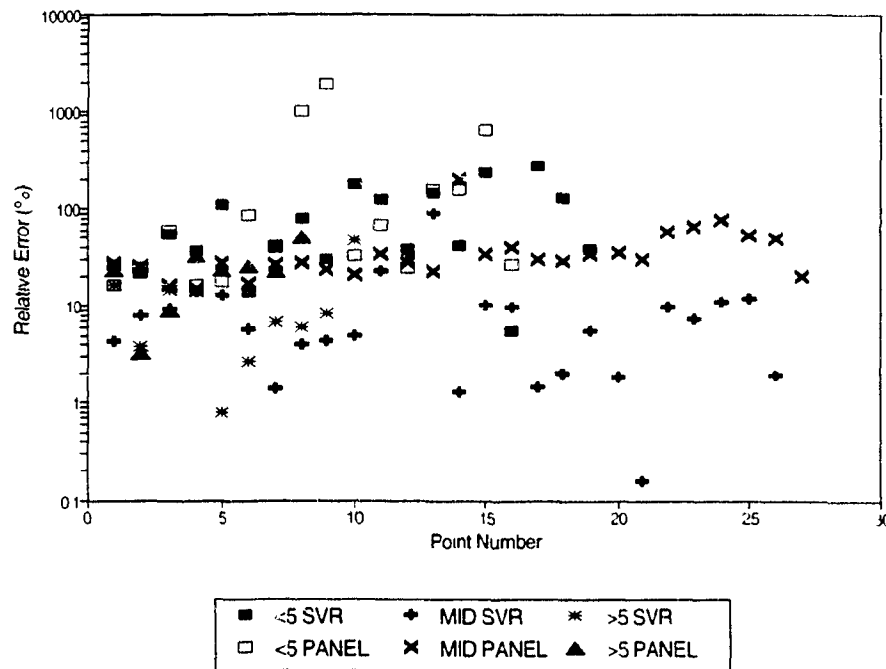
#### **4.3.6 RELATIVE ERROR AND POSITION IN THE CROSS-SECTION**

Figure 4.6 is a plot of relative error as a function of location in the profile for CS9. Each profile has been divided into 3 zones: zone 1, identified as <5, is the near bed zone, and consists of those points located at 0.025 and 0.050 m off the bed; zone 2, MID, are those points located between the near-bed zone and the points closest to the surface; zone 3 is the near-surface zone and consists of those points closest to the surface.

From the Figure (4.6) it can be seen that the highest

relative errors are in zone 1. The values for zones 2 and 3, for the panel removal runs, are higher than the corresponding values for the single value removal runs. This shift in magnitude for zones 2 and 3, and to a lesser extent zone 1, is apparent for all cross-sections.

**FIGURE 4.6 RELATIVE ERROR AS A FUNCTION OF LOCATION IN PROFILE CROSS-SECTION 9**



The labels <5, MID and >5 refer to the 3 zones (see text). SVR represents the points involved in the single removal of points and PANEL refers to the runs in which all the points in a panel were removed. The largest errors are in the near bed region for all cross-sections (CS) presented here e.g. point numbers 8,9 and 15).

#### 4.3.7 MULTIQUADRICS AND VELOCITY PROFILES

The shapes of the velocity profiles (the term velocity, as used above and in the following discussion, refers strictly to the speed of the flow, and not the direction. To be consistent with the literature, the term velocity profile is used in this thesis, but does not relate to the vectorial component of flow) based on the original known data points and those based on the interpolated data, both the data from the SVR and the panel removal runs, are different. The profiles based on the original data tend to be irregular in shape, reflecting the differences in fluid speeds throughout the vertical. The profiles based on the interpolated data tend to be more linear and less irregular.

The profiles can be grouped into 3 general categories. The profiles constructed from the sampled fluid speeds are irregular and show rapid changes in fluid speed over short vertical distances. Profiles based on interpolated data when single points are removed tend to be linear between the 2 known points that are around the removed point. In other words, the interpolant is a point that lies on a straight line between the 2 known, nearest neighbours points. The last category is for the profiles for runs in which only the points on the convex shell were used as the input data set. These profiles are linear.



For the single value removal runs, the magnitude of the error associated with the interpolated profiles will depend largely on the shape of the original profile. If sections of the original profiles were linear, then the errors will be small. In the case of the panel removal runs, the shape of the profile is always linear, regardless of the shape of the original profile.

Figure 4.7 shows 5 velocity profiles for panel 5, CS8. The line labelled 8, with solid squares as the symbol is the velocity profile based on the original data points. The profile is very irregular. The profiles labelled 8-1 and 8-2 represent the curves for the runs in which the even and odd numbered points were removed from the data set respectively.

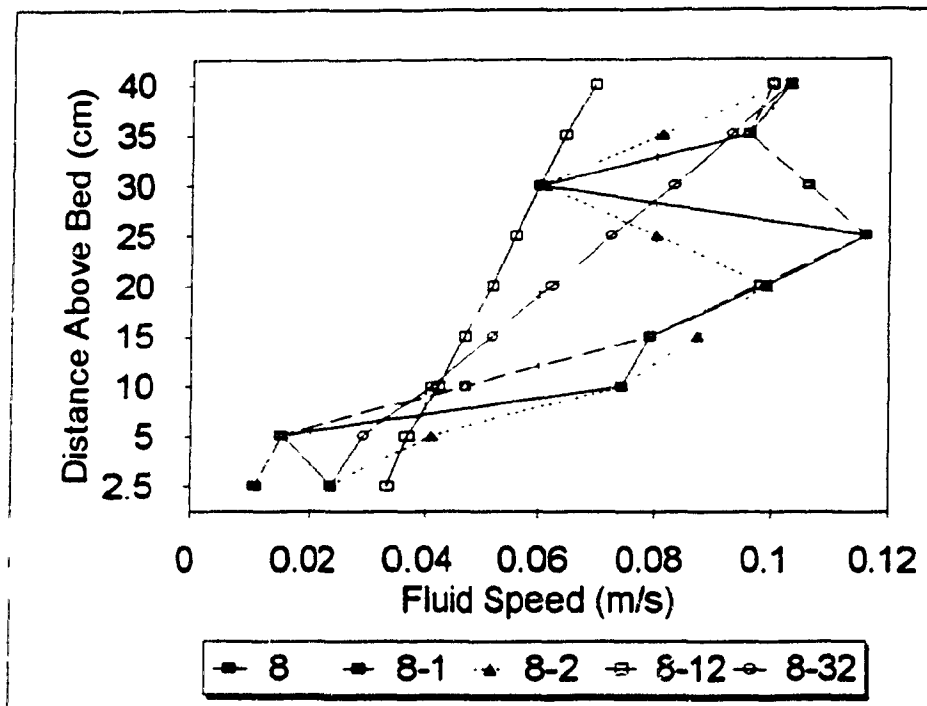
From the curves for 8-1 and 8-2, it can be seen that the interpolated values for single points lie in the middle of the straight line segment between known points. An example of this can be seen in the upper right corner of the graph. For run 8-2, the point at 35 cm above the bed was removed. The point interpolated for this point is the average of the points at 25 and 35 cm above the bed.

The remaining 2 curves, labelled 8-12 and 8-32, are for the panel removal runs. Both curves are straight lines. For 8-32, the bed and surface points were used in the set of input points. The values interpolated for the points in between are on the straight line segment between the bed and surface

points.

The influence of the nearest neighbours is very evident from the velocity profiles. In the runs in which single values were removed, the interpolated point is in the middle of the line between the nearest neighbours.

**FIGURE 4.7 VELOCITY PROFILES - PANEL 5, CROSS-SECTION 8**



The curve based on the original data (labelled 8 with solid black squares) is irregular in shape. The profiles 8-1 and 8-2 are for the runs in which every even or odd point were removed. The interpolated values lie on the straight line between the 2 known nearest points. The last 2 profiles, 8-12 and 8-32 are for the panel removal runs.

For the panel removal runs, there appears to be a distance-limiting influence. This means that the closer to the known panel a vertical is, the more the shape of the profile will resemble that of the known profile. As you move away from that profile, the shape of the interpolated profiles become less and less like the known vertical and more linear. Figure 4.8 is a plot of the velocity profiles in the area of panel 6, CS8 for run 8-13 (odd numbered panels were removed).

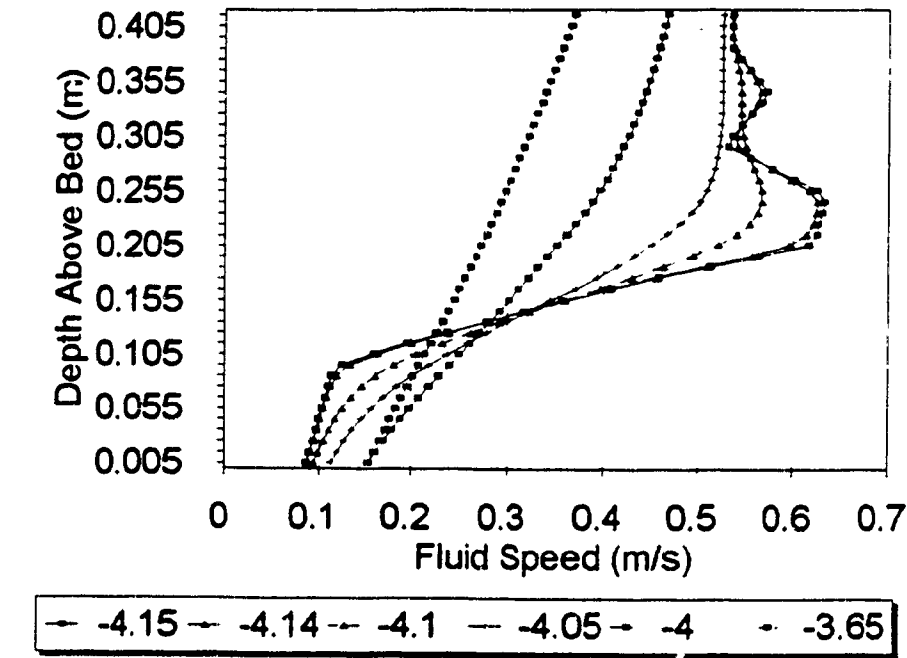
Panel 6, with the original data points is at -4.15. The curve 1 cm over, -4.14 is nearly identical to that at -4.15. As you move away from the known panel, the shape of the curves begins to change so that they look less and less like the one for panel 6. Eventually you reach a point in which the profile is a straight line (in the Figure this is around -3.65).

For the same run described above (odd numbered panels removed), the velocity profiles are shown for the area around panel 5 (Figure 4.9). The known panel is located at -3.40. The profiles for 0.05 m on either side are also displayed. It can be seen that for panel removal runs, the profiles closest to the known panels resemble the shape of the panel profile. As you move away, the shape changes until it becomes linear. If the profiles in the area of panel 4 were displayed for the same run, the same pattern seen at panel 6 would appear, except that the panels would become straighter as you

moved to the right (in Figure 4.8 the curves become straighter as you move to the left). At some distance away from the known panels the velocity profiles are straight lines (Figure 4.8 and Figure 4.9).

For this series of analyses, the run in which the removal of the numbered panels, the distance at which the interpolated profiles become linear is between 0.25 m and 0.30 m away from a known panel. This value is based on the observation of the graphed profiles in this analysis.

**FIGURE 4.8 VELOCITY PROFILES FOR PANEL 6, CROSS-SECTION 8, PANEL REMOVAL RUN (R813)**

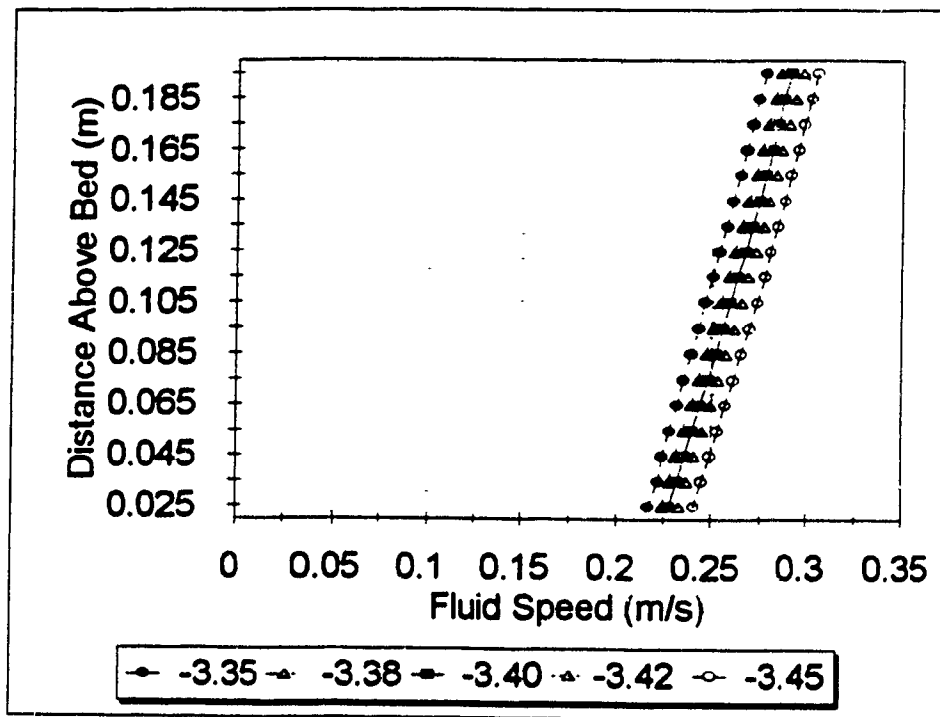


-4.15 is the profile based on the original data at panel 6. The profile for the vertical 0.01 m and 0.05 m to the left of panel 6 are labelled -4.14 and -4.10, respectively. The remaining three panels represent the profiles for 0.10 m, 0.15 m and 0.40 m to the left of the known panel, 5. The profile -4.14 is nearly identical to that of the known vertical, -4.15.

#### 4.3.8 MULTIQUADRICS AND THE NO-SLIP CONDITION

The speed at the point where a fluid is in contact with the boundary is the same as that of the boundary; in other words, the velocity will be zero. This condition is known as the no-slip condition (Middleton and Southard, 1984). In a river, this point is located at the bed/fluid interface.

FIGURE 4.9 VELOCITY PROFILES FOR PANEL 5, CROSS-SECTION 8,, R813



In this analysis, the odd numbered panels have been removed. The profiles

are based on the interpolated data and are in the area of panel number 5. This panel has been removed. The panels in the area between the known panels (ie. numbers 4 and 6) are linear (Figure 4.8 for the area around panel 6).

To make use of the no-slip condition, a fluid speed of 0 m/s was placed at a point 0.001 m below the bed of the river (e.g. if the depth of flow was 0.29 m, the Y coordinate for the no-slip test was 0.291 m). By placing the point immediately below the river bed, the fluid speed was guaranteed to be 0 m/s (it was assumed that flow from ground water was negligible and therefore had no influence on the downstream component on flow). The sampled point at 0.025 m above the bed was then removed and interpolated. Table 4.10 summarizes the result of the no-slip test for CS10.

**TABLE 4.10 RESULTS OF NO-SLIP CONDITION TEST: CROSS-SECTION 10**

Panel #	Known Speed (m/s)	Int. Speed (m/s)	AE (m/s)	RE (%)
1	0.147	0.085	0.062	42.18
2	0.103	0.112	-0.009	-8.74
3	0.091	0.089	0.002	2.20
4	0.232	0.120	0.112	48.28
5	0.102	.0082	0.020	19.61
6	0.117	0.093	0.024	20.51
7	0.061	0.039	0.022	36.07
8	-0.021	0.018	-0.039	185.71
9	0.025	0.073	-0.048	-192.00

10	0.008	0.043	-0.035	-437.50
----	-------	-------	--------	---------

The interpolated speed, column 3, is approximately equal to the value of the speed at the point 0.05 m above the bed divided by 2. The calculation of this value is the same as that used to derive the interpolant in the single value removal and for the values between the surface and bed points used in the panel removal runs. In other words, the values are in the middle of the line segment connecting the 0 m/s point and that at 0.05 m off the bed.

At panel 8 the known speed was -0.021 m/s. The interpolated value was 0.018 m/s. The fluid speed at the point immediately above this removed point was 0.035 m/s. Similar to the results from the SVR runs, in areas where there is reverse circulation at the bed, but not at the point above it, the interpolated value appears as forward flow (i.e. moving downstream).

#### **4.4 DISTRIBUTION OF ERROR - PLAN VIEW - SVR**

##### **4.4.1 RELATIVE ERROR**

###### **4.4.1.1 BED SPEEDS**

The largest relative error was -27100.00 %, which was

located at panel 1, CS8. At that point the known speed was 0.001 m/s and the interpolated value was 0.272 m/s. Cross-section 7 had 1 panel, 3, with an error over |100.00 %| (-3120.00); number 8 had 5 panels, 1,3,7, 8 and 10 over 100.00%; CS9 had 3 panels over 100.00 %, 1, 2 and 5 while panels 1 to 3 at CSs 10 and 11 all had values in these large error classes.

#### **4.4.1.2 SURFACE SPEEDS**

The areas with the largest relative errors in the surface analyses were: panel 3, CS 7; panels 1,6, 8 and 10 at number 8 and panels 1 to 10 at CS9 to CS11. The cross-section with the lowest values were 9 and 10, with the lowest value being 0.32 % at panel 5, CS10. Of all the cross-sections, number 8 had the largest relative errors.

#### **4.4.1.3 AVERAGE SPEEDS**

Cross-section 8 had the most number of panels, 3, with errors over |100.00 %|. Cross-section 7 has 1 value over 100.00 %, panel 1, while the rest of the panels had values concentrated between classes 25.00 to 50.00 %. The largest values for CS9 to CS11 were at panel 1; however, the value at panel 1, CS10, was much lower, 58.75%, compared to those at



number 9 and 11, 258.33 % and 2300.00 %, respectively. The relative errors in the average analyses are predominantly in the 20.00 to 40.00 % classes (Figure 4.10A).

#### **4.4.2 ABSOLUTE ERROR**

##### **4.4.2.1 BED SPEEDS**

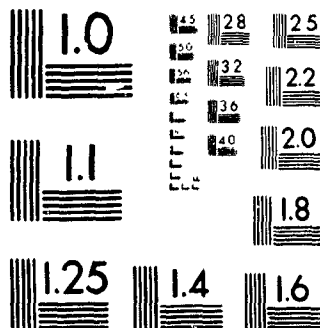
The largest absolute errors for this set of analyses are at CS7 and CS8, with those at panels 1 to 3 CS8 being the largest. Panels 4 to 10, at number 8 were all below 0.050 m/s. Cross-section 11 had the lowest absolute errors of the 5 cross-sections. Of the 49 interpolated points, 24 were over-estimates, with varying magnitude.

##### **4.4.2.2 SURFACE SPEEDS**

The largest differences between the known speeds and interpolated speeds for all the cross-sections were located at the ends of the cross-section; that was, at panels 1, 10 or both. Panel 1, CS8, had the single largest value of any of the plan view analyses (including both panel and svr runs), with a value of -0.847 m/s. Of the 2 points that had known speeds with a negative value, panels 9 and 10 at CS8, one had an interpolated value that was also negative.

2 of /de 2

PM-1 3 1/2"x4" PHOTOGRAPHIC MICROCOPY TARGET  
NBS 1010a ANSI/ISO #2 EQUIVALENT



#### **4.4.2.3 AVERAGE SPEEDS**

From figure 4.10b, it can be seen that errors associated with these analyses are located mostly in the 0.020 m/s to 0.25 m/s classes, with the modal class being 0.100 m/s to 0.150 m/s. The area with the largest absolute errors was CS 7 - only 2 of the 9 panels were within 0.090 m/s of the known speeds. At CSs 8 to 11, the largest values were located along the outside edge of the bend (i.e. along the upstream left part of the river).

FIGURE 4.10A AND B - ERROR DISTRIBUTION - PLAN VIEW - SVR

FIGURE 4.10A RELATIVE ERROR

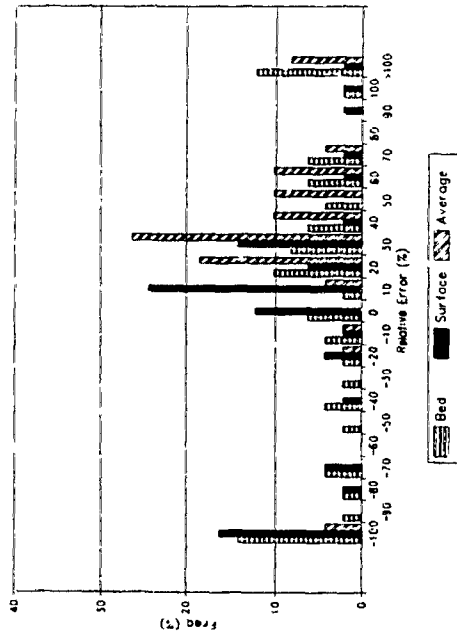
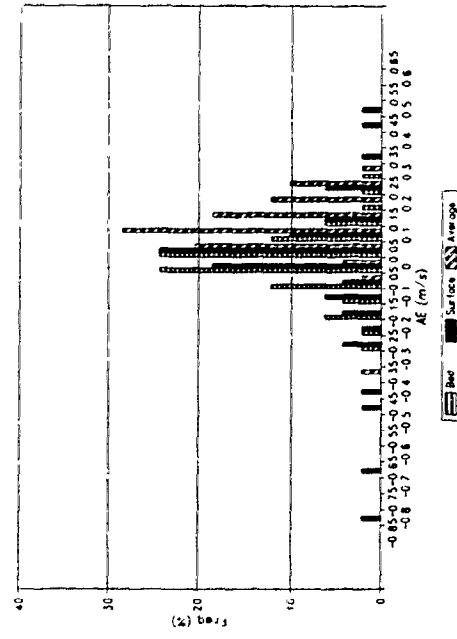


FIGURE 4.10B ABSOLUTE ERROR



#### 4.4.3 DISCUSSION

The location of the extreme values, particularly the relative errors, can be grouped into 3 overlapping categories: in areas of reverse flow, in areas of steep fluid speed gradient and areas located along the upstream left side of the channel (i.e. the outside of the bend). All directions, left or right, are referenced to the upstream left bank.

The high relative errors associated with panels 8 to 10 at CS8, panels 2 and 5 at CS9 and at panel 3 at number 10, are in areas of reverse flow. When these single points were removed, with the exception of panel 8, CS8, the interpolated values were all positive, the same sign as the nearest fluid speeds in these cross-sections.

In the area around panel 3 at CS7 and CS8 there was a rapid deceleration in flow; in other words, the speed at these points was much smaller than the surrounding points. This area, then, had a steep fluid speed gradient. When these single points were removed, the interpolated values were much larger than the known points.

The largest value at CS11 was located in the first panel. The panels located closest to the upstream left bank tended to have larger errors than those panels that were not in areas of reverse flow and that were not located near the ends of the

cross-section. This pattern of larger errors at panel 1 and 10 may be due to the fact that these points lie on the edge of the convex shell of known points. This means that interpolated values were in fact extrapolations.

Also, the area along the outside of a bend was the area of maximum fluid speed. As a result, when points located in this area were removed, interpolated values were markedly different due possibly to the fact that the nearest points may not have been close in magnitude.

#### **4.5 DISTRIBUTION OF ERROR - PLAN VIEW - PANEL RUNS**

##### **4.5.1 RELATIVE ERROR**

###### **4.5.1.1 BED SPEEDS**

Of the 40 points interpolated in the 2 combined bed analyses, 13, or 32.5 % had relative errors over  $|100.00\%|$ . Cross-section 8, near the entrance to the bend (Figure 2.1b), had 6 panels with errors over 100.00 %. Panel 1, located at the closest point near the upstream left channel bank, and panels 7-10, located near the upstream right channel bank, were the locations of these errors.

Cross-section 9 had 2 panels, numbers 2 and 5, with an absolute error value over 100.00%. Panels 1 and 3, along the

outside of the bend, at CS10 had values over 100.00%, while panels 1,3 and 4, at CS11, all had errors over 100.00%. Between panels 1 and 3 at number 11, panel 2 had a relative error between 90.00 and 100.00 %.

Cross-section 8 had the largest relative error of the bed fluid speeds when all the points at the panels were removed. The largest errors in the panel removal runs occurred at the panels located at the beginning and end of the cross-sections (i.e. 1 and 10). The bimodal distribution of Figure 4.11a was due to the extreme error values located at the margins of the cross-sections.

#### **4.5.1.2 SURFACE SPEEDS**

Cross-section 8 had the largest relative errors of the four cross-sections for surface speeds. Panels 1, located at the upstream left side of the channel, and panels 6 to 10, which extended from mid-channel to the upstream right bank, had the largest relative errors (4 of the 5 panels had values over 1000.00 %).

The relative errors at CS9 to CS11 were smaller than those associated with CS8. Only 1 panel, number 1 at CS10, had a value over 100.00 %. Cross-section 10 had the lowest relative error of the 4 cross-sections. Panels 2 to 4 and 9 had errors between 0.0 % and 10.0 %, with 4 panels having

values between 10.0 % and 20.0 %.

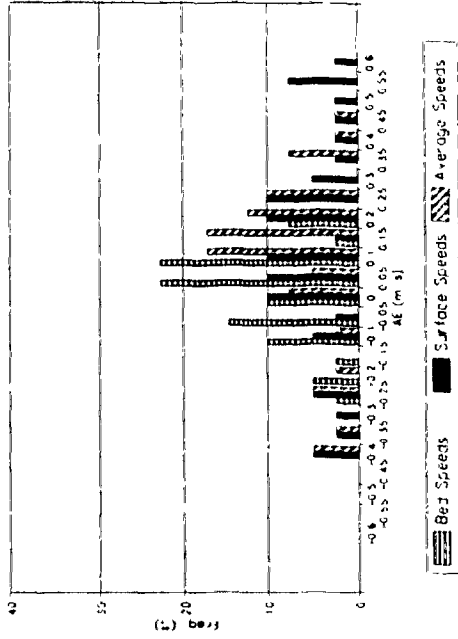
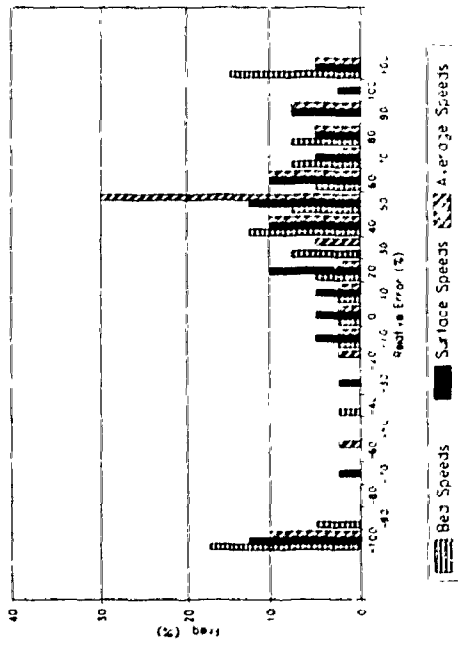
#### **4.5.1.3 AVERAGE SPEEDS**

Six of the 40 interpolated average speeds had relative errors over 100.00%. Of the 6, 5 were located at CS8. Panels 1 and 7 to 10 had the largest errors. All were greater than 100.00 %, with those at panels 8 to 10 greater than 1000.00%. Cross-sections 9 to 11 show a concentration of errors between 40.00% and 60.00% (Figure 4.11a). Cross-section 11, panel 1, was the only other panel/cross-section with a relative error over 100.00%.



FIGURES 4.10A AND B - ERROR DISTRIBUTION - PLAN VIEW - PANEL RUNS

FIGURE 4.10A RELATIVE ERROR



## **4.5.2 ABSOLUTE ERROR**

### **4.5.2.1 BED SPEEDS**

The largest absolute errors for CSs 8 are located at panels 7 to 10, with values of -0.194 m/s, -0.211 m/s, -0.241 m/s and -0.252 m/s. These four values are also the largest absolute errors of all the cross-sections for this set of analyses. Cross-sections 9 and 10 have the lowest absolute errors with values in the classes between 0.0 m/s and 0.100 m/s. Panels 1 and 3, at CS11 have absolute errors of -0.131 m/s and -0.119 m/s. These values, in addition with a difference of 0.174 m/s at panel 7, CS10 are the largest, in addition to those associated with CS8.

### **4.5.2.2 SURFACE SPEEDS**

Cross-sections 8 and 9 have the largest absolute errors of the 4 cross-sections. The largest values - 0.567 m/s, 0.541 m/s, 0.531 m/s and 0.527 m/s are located at panels 2 and 4 at CS8 and panels 2 and 3 at number 9, respectively. These panels are located along the left hand side of the channel, corresponding the outside edge of the bend. Panels 8 to 10, at CS8, also have large differences (large compared to those values at panels 10 and 11). The smallest values are located at panels 2 to 9 at CS10, with values ranging from 0.002 m/s

to 0.063 m/s (the values at panels 1 and 10 at this cross-section are -0.137 m/s and -0.121 m/s, more than double the value of 0.063 m/s).

#### **4.5.2.3 AVERAGE VALUES**

The single largest value was 0.427 m/s at panel 3, CS9. Overall, the largest differences in this set of analyses are located along the upstream right hand side of the channel at CS8 (panels 8 to 10) and at panels 2 and 4 at CS9. There are no values within +/- 0.110 m/s of the original speeds at CS8. Cross-section 10 has the most number of panels within the lowest absolute classes (Figure 11b).

#### **4.5.3 DISCUSSION**

There was a shift in the magnitude of absolute errors from the bed to the surface speeds to the average speeds. The bed speeds are concentrated in the classes +/- 0.100 m/s, while the surface errors shift towards 0.050 m/s to 0.150 m/s. The errors associated with the average speeds are greater than those in the surface and bed runs.

Cross-section 8, especially at panels 7 to 10, had the largest errors for both the relative and absolute errors. This was particularly true for the analyses of bed speeds. The average fluid speeds, as well as the bed speeds, in this

area of CS8 were negative, indicating reverse flow. For the surface speeds, the values were positive. In terms of the interpolated fluid speeds at CS8, none were negative.

The large relative errors associated with panels 2 and 5 at CS9 and at panel 3, CS10, were also negative. Again, the values interpolated for these points when all the panels were removed were positive.

In addition to the largest errors occurring in areas of reverse flow, a general pattern of large errors being located at the ends of the cross-sections (near panels 1 and 10) was also present. A plausible explanation for this pattern might be that these panels were located closest to the channel banks, and as such, tended to have fluid speeds that were different from the interior points (interior meaning between panels 1 and 10). When these points were estimated, using all the other points, the errors were larger because of the difference in known speeds between the end panels and the midpanels.

## CHAPTER 5: DISCUSSION

### 5.1 VELOCITY PROFILES AND MULTIQUADRICS

Leopold et al. (1964) and Nordin (1963) showed that velocity varies logarithmically away from the bed, with the greatest speed located at a position near, but not at the surface. Chow (1959) demonstrated the influence that roughness has on the velocity profile - the curvature of the profile increases because of material on the bed (see his fig. 25, p 25). Savini and Bodhaine (1977) found that the upper 95% of their data could be described logarithmically, but that the lower 5% could best be described by a power function because the velocity changes more rapidly in the lower portion of the curve where bed and bank roughness causes turbulence and fluid speed variation (Morisawa, 1985).

Bridge and Jarvis (1977), working on the River South Esk, and Saunderson and Lockett (1983), using flume data with a rippled bed, found that velocity profiles over these bedforms were not logarithmic. Hickin's (1978) velocity profiles for the Squamish River were very irregular. Robert et al. (1992) showed that different types and sizes of bed roughness elements can increase turbulence and cause variation in fluid speed.

The profiles based on the original data points (line - 4.15, Figure 4.7 as an example) are very irregular in shape.

The data could not be described logarithmically. This can be expected from data collected in natural channels and for flumes with rough boundaries. The near bed velocities in the data sets were, in many cases, markedly different from those in the upper areas of flow. Given the depth of flow, and the size of the roughness elements, it is not surprising that velocity profiles show rapid changes in speed both near the bed and in the upper parts of the profile.

Using the multiquadric technique of interpolation, the velocity profiles tended to become more linear. First, when single values were removed, the interpolated value was very close, and in most cases the same as the mean value of the two nearest neighbours. For the panel removal runs, the velocity profiles in the region of the removed panel were straight lines (Figure 4.8). As one moved closer to the known panels, the shape of the velocity profiles became closer to that of the known profile (Figure 4.7).

Based on these observations, and the absolute and relative errors associated with these interpolations, the multiquadric technique failed to accurately represent the fluid speeds. This was particularly true in areas where there was a rapid change in speed and in areas of reverse flow. Near-bed points (i.e. 0.025 m off the bed) were often in zones of reverse circulation, while points immediately above them were in areas of downstream flow. When the points in these reverse circulation zones were removed and interpolated, the

multiquadrics did not accurately represent the fluid speed track.

This situation is similar to that experienced in some of the applications to topography. If areas of highs and lows, ridges and saddles, were not adequately sampled, the topographic surface generated by the multiquadrics did not accurately represent the true surface. The solution for the studies of topography using map data was to simply increase the density of points in these significant areas. For fluid speeds, the solution is not as simple.

It is hard to predict which areas of the channel will have flow that is different from other areas, including points in the same vertical. A visual inspection of surface velocities may be not be useful because the fluid speed pattern near the surface may completely differ from that below the surface and at the bed. This can easily be seen in the velocity profiles for this study, and in those listed above.

The velocity profiles were created using the surface technique of interpolation. Multiquadrics can also be used for curve fitting. Carlson and Foley (1992) used multiquadrics and a number of other interpolating routines for track data - sea temperature irregularly sampled along tracks. They concluded that of the techniques tested, multiquadrics worked the best for track data.

The equation for curve fitting is (Sirayanone, 1988, p. 8):

$$(14) H_j = \sum_{j=1}^n c_j |X_1 - X_j|$$

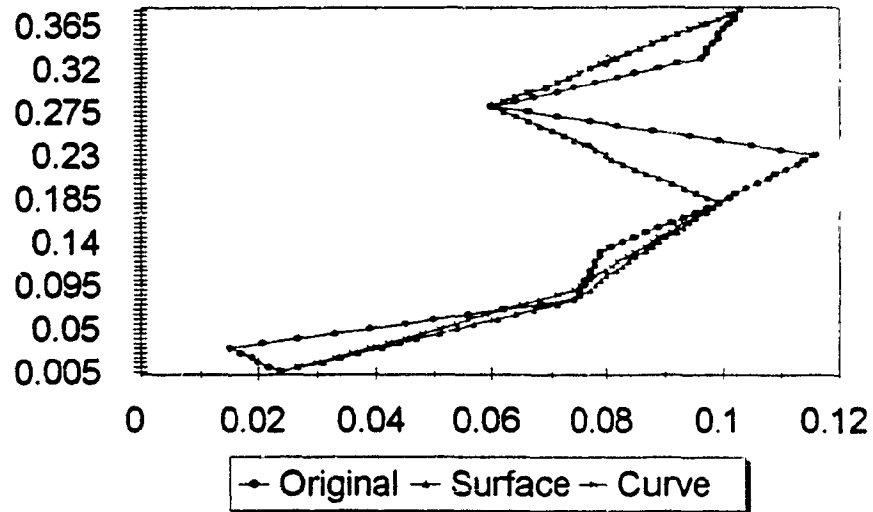
Recently, Saunderson (1994b) presented graphic results using multiquadric curve fitting to a number of different data sets, including float tracks in the Gulf Stream and in the Sub-Tropical Gyre. The results showed that the curve passed through the original control points exactly.

A test file using data from panel 4, CS8 was run by Saunderson for this study. In this test file 4 points were removed from the vertical. This curve was compared against the curve generated using multiquadrics and all 59 data points in CS11 (control curve) and against a curve generated using all the data in the original file, with the exception of the 4 points removed in the curve fitting test file (N=55). The results are displayed in Figure 5.1.

The profile generated using the curve fitting routine (labelled curve in Figure) and that based on the surface technique with the same 4 points missing are nearly identical in the lower portion of the graph; in the area above 0.150 m the curves are identical. Each of these 2 curves created straight line segments between the known sampled points. Neither profile accurately represents the true data.



**FIGURE 5.1 MULTIQUADRICS AND CURVE FITTING: PANEL 4,  
CROSS-SECTION 8**



The data for the curve profile came from an analysis performed by Saunderson on the data from panel 4, cross-section 8.

## **5.2 COMPARISON OF CROSS-SECTION AND PLAN VIEW ANALYSES**

There is a general shift in the magnitude of relative error from the cross-section analyses to the plan view analyses. The errors associated with the bed, surface and average fluid speeds associated with the plan view are larger than the errors from the cross-section analyses.

The relative errors for the single value removal runs (SVR) in the cross-section analyses are the lowest of all the relative errors. The errors for the panel removal runs for the cross-section data are larger than the SVR errors. The relative errors for the plan view are larger than the cross-section errors.

The number of relative errors over 100 % (both positive and negative) is greater in the plan view than in the cross-section view. This is especially true for the bed fluid speeds. The bed speeds in the plan view are concentrated in the first and last classes.

A visual examination of the figures shows the shift in error magnitude between the two types of analyses, which could be the result of larger distances between nearest neighbours. In the cross-section analyses, the distance between points in the same vertical were on the order of centimetres, while the distance between adjacent panels was on the order of 1-3 metres.

In the plan view the distance between adjacent points at a cross-section was on the order of tens of centimetres to a few meters. The distance between cross-sections was on the order of several to tens of metres.

### 5.3 SAMPLING PROCEDURES

One of the important uses of fluid speed data is the study of particle movement - both bed load and suspended sediment. The near bed velocity is considered to be of primary importance in the initiation of particle movement (e.g. Fortier and Scobey, 1926); while other studies use a mean fluid speed (e.g. Komar, 1987). For this reason it is important to get an accurate picture of the distribution of fluid speed across and through a reach. Within the same cross-section there are areas of aggradation and degradation. If incorrect inferences are made about the distribution of fluid speeds, then models and equations used to predict sediment using fluid speed will be incorrect. A complete image of fluid speed patterns is needed in the study of sediment movement. The use of interpolating procedures is one way by which a larger picture of fluid speed can be determined based on a limited number of control points.

The testing of the no-slip condition was an attempt to determine if using a theoretical fluid speed value could be used to accurately represent this near bed region. An accurate representation of fluid speeds based on this value would reduce the need for increased sampling in this region.

The results show that the use of 0 m/s at the bed does not accurately represent the bed either visually or quantitatively. A possible explanation for this is that the

point at which the no-slip conditions occur may be on the molecular level. This would mean that placing a value of 0 m/s just below the surface of the bed may not accurately represent the real situation. Another explanation is that the point of 0 m/s did occur at the selected point, but that the rate of change was so great in such a small distance that it would have been impossible to accurately sample points in this space. To test this idea, a way of measuring fluid speed at the millimetre, or micrometer level may be needed.

Because the interpolated values tended to be linear, an increase in sampling density is needed to increase the level of accuracy and reduce the magnitude of the errors involved. Given the width and depth of the study reach, the sampling procedure employed may be considered detailed or fine. Given the magnitude of the errors involved, it appears that the sampling density selected was too low for the procedure.

As mentioned before, when this problem arose in testing multiquadrics with data from map sheets, the solution was to select more points in the significant areas. For studies of fluid speeds, this means increasing the number of points, particularly in the near bed regions and areas with a low relative roughness value.

#### **5.4 BED ROUGHNESS AND TURBULENCE AND MULTIQUADRICS**

The largest relative errors are in the bed and near bed

zone (fig. 4-6). Leighly (1934) discussed the theoretical distribution of velocity and turbulence for both symmetrical and asymmetrical channel cross-sections. The zone of maximum velocity is located just below the surface, while the zones of maximum turbulence occur along the bed, close to the sides away from the midpart of the channel. The influence of bed material is greatest in the near-bed area. The role, or influence that bed material will have on the distribution of velocity and turbulence is a function of both the depth of water, and the size of the particles.

To determine geomorphological explanations for the pattern of errors associated with multiquadrics, the relationship between bed roughness and turbulence, average relative error was plotted as a function of relative roughness and Reynolds number.

Relative roughness is the ratio of the depth of flow to particle size:

$$(15) \quad R_r = d/D50,$$

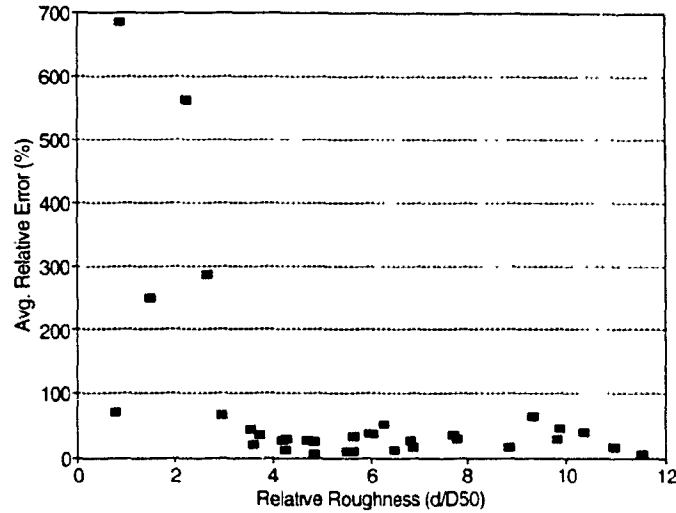
where  $R_r$  is the relative roughness,  $d$  is the flow depth and  $D50$  is the mean B axis of the measured particle size (chapter 2). In figure 5.2 each point on the graph represents the relative roughness for each panel at each cross-section at which particles were measured (recall that because of the nature of the bed in some areas, some areas were not sampled). The relative error value is based on the average for the runs in which the even and odd points were removed.

A relative roughness close to 1 means that the particle is equal to the depth of flow; as the value for  $R_r$  increases, the depth of flow is much larger than the mean particle size.

From Figure 5.2, the 5 largest average relative error values are at the panels with the largest relative roughness value (the closer the relative roughness number is to 1, the larger the value). When the particles were selected off the bed, an attempt was made to sample the entire panel, in a random fashion. This means that particles beneath the transect line, in addition to in front of and behind the line were measured. To represent this area, only 5 particles were used. It is possible that if a larger sample had been taken in a more systematic procedure, particularly in the area in front of the transect line, the relationship between the two might have been stronger.

Fluid speeds were taken at points in the vertical; the influence of particles in front of the transect line could be seen in the profile, but may not have been sampled in the measurement of particles. In other words, the error value associated with particular points in the vertical may have been more a function of roughness elements in the area upstream of the sampled space.

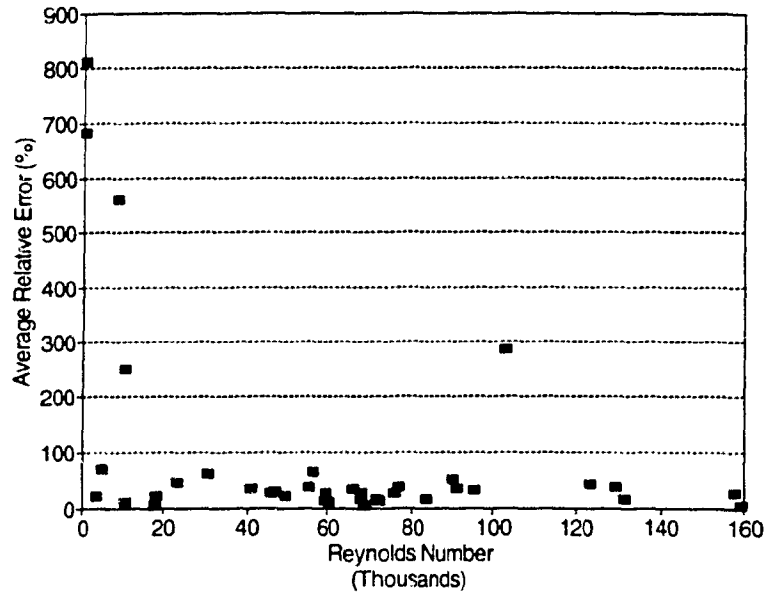
FIGURE 5.2 RELATIVE ROUGHNESS AND AVERAGE RELATIVE ERROR



The Reynolds number can be used as a measure of turbulence (Leopold *et al.*, 1964; Morisawa, 1985). The Reynolds number was calculated for each panel using the depth of flow at the panel, the mean velocity for the panel and the temperature recorded for the entire cross-section (table 2.2).

The higher the Reynolds number, the greater the turbulence. In Figure 5.3, the highest relative errors are at the lower Reynolds number. This is contrary to what one would expect.

FIGURE 5.3 RELATIVE ERROR AND REYNOLDS NUMBER



One explanation for this might be the use of the Reynolds number as an indicator of turbulence. It is possible that a another parameter of turbulence intensity might be better. Another parameter used to describe turbulence is the root mean square of the velocity (Middleton and Southard, 1984). The root mean square error for the cross-sections were calculated and mapped. The distribution of these errors was very irregular, with locations of maximum turbulence being located throughout the profiles. As a result, it was decided not to use this parameter as a measure of turbulence and error value.



Another possible explanation is that the method used to calculate the Reynolds number gave the value for a point in the channel when in fact, turbulence is not an at-a-point phenomenon. Turbulence is the result of interactions between fluid speed, depth, roughness and channel geometry throughout an area, not just at one point. Therefore, the value for the Reynolds number calculated at a point may not accurately reflect the cross-section or reach as a whole. An average Reynolds number based on consecutive cross-sections plotted against an average relative error for the same cross-sections might have revealed a better relationship.

One factor not considered in this study, but one that would have an impact on turbulence and fluid speed pattern, is the influence of stage. A change in water level can influence the fluid pathways, particularly in meanders (Hey and Thorne, 1975). As stage rises, the relative roughness decreases, meaning the influence of the bed particles may become drowned out (Leopold and Wolman, 1960; Hey and Thorne, 1975 and Robert *et al.*, 1992).

Given changes to fluid speed patterns, and the potential dampening effect of bed elements, it would be desirable to test the multiquadric technique of interpolation using data collected over various stages. It is possible that at higher flows in gravel bed rivers, multiquadrics may more accurately represent fluid speed than it did during base flows.

## CHAPTER 6 CONCLUSIONS

### 6.1 SUMMARY

Big Otter Creek, a gravel bed river, was sampled for fluid speeds to use as input data for the multiquadric method of interpolation. The cone model was the only quadric used in the study.

Fluid speeds were sampled at various verticals across the channel and at different locations within the vertical . An electromagnetic current meter was used to sample the speeds. A total of 10 readings was taken at each point in the vertical and averaged out to give a point mean speed. At each cross-section depth and bed material was measured to determine the relative roughness.

The goal of testing the multiquadric technique of interpolation was achieved by systematically and randomly selecting and removing points from the cross-section and plan view data sets. The objectives of identify the magnitude, distribution and patterns of the errors were achieved by calculating the absolute and relative errors, plotting the histograms for these errors and examining error magnitude as a function of position in the vertical and channel. Geomorphological explanations for the errors were examined by plotting error value as a function of relative roughness and Reynolds number. Fluid speed sampling procedure was looked at

by analysing the error values when the number of control points, and their position was changed, and by testing the no-slip condition.

The results indicate that the multiquadric surface based on the cone model represented the known control points exactly, but that when speeds were interpolated between known points, the surface did not accurately represent the fluid speeds. This was particularly true in areas with steep fluid speed gradients - the location of the largest errors were in these areas.

Also, the velocity profiles based on interpolated points tended to be linear in shape. When areas of the cross-section were interpolated between known panels, the velocity profiles were linear. Within a certain distance of a known panel, the interpolated fluid speeds, as indicated by the velocity profiles, resembled the shape of the known points. As the distance away from these known panels increased, the shape of the interpolated profiles resembled less and less the known profile and became more linear. In rivers, however, velocity profiles are rarely straight lines.

Although the technique used was a global procedure, the nearest neighbours had the greatest influence on the interpolants. To describe a vertical, a local interpolation procedure may be better. From the panel removal runs, there appears to be a distance beyond which the influence of the known fluid speeds decreases and the velocity profiles become

straight lines. In other words, the influence of nearest neighbours is seen both within a vertical and in the area surrounding the vertical.

A comparison was made between the curve fitting technique using multiquadrics and the surface fitting technique. Although the test was run only on a very small sample, there appears to be little difference in the value of the interpolation between the two procedures. A possible explanation for this is that the distance between consecutive verticals is too large in the global procedure. Due to this large distance, the influence of fluid speeds outside some critical distance around known points became zero.

This results of the test indicates that a local procedure of interpolation might be more suited to this data set than the global method. By reducing the distance between known points, the quality of the interpolants, as indicated by the error value, should increase.

Two sampling procedures were used to select control points - a systematic and a random approach. Included in each was a variation of the number of control points. Overall, the total number of control points was less critical than the location of the control points.

Despite the reduction in the number of control points by as much as 50%, the value interpolated for a single point did not change across the various runs. The value did change when a point immediately above or below was removed (table 4.9).

An example of this can be seen in the second type of random removal runs. The value interpolated for point 28 did not change as the number of control points decreased unless the points immediately above or below were removed.

Control point density, especially in areas of reverse flow, appears to be a crucial factor in the effectiveness of the interpolating routine. In areas where there is a rapid change in fluid speed, more points are needed to accurately represent the surface.

The velocity profiles show that the fluid speed is very irregular, especially in the area of the bed. There were patterns of error associated with the techniques. The magnitude of the errors associated with the panel removal runs was larger than that for the single value removal runs. For both types of analyses, the largest errors were in the boundary region, especially in the near bed region.

The errors associated with the plan view analyses were larger than the those with the cross-section analyses. A general hierarchy of error can be established. The lowest errors were for the analyses in which single values were removed (SVR) from the cross-section data sets. The second level in the hierarchy is the error related to the removal of all the points from the panels/all points except those along the convex shell in the cross-section runs. The plan view analyses had the largest concentration of errors in the higher error classes (figures 4.10 and 4.11).

The magnitude of the errors increased when the distance between sampled points increased (the distance between nearest cross-sections in the plan view runs was larger than the distance between adjacent panels in the cross-section analyses).

This thesis tested the cone model as a method of interpolation using data collected at points off the bed at 10 panels located across the channel and throughout the reach. To improve the quality of the interpolation using the cone model, a greater density of control points appears to be needed.

An alternative approach would be to test different surfaces with the same data set. This would involve using values other than 0 for  $C$ , or could involve using hyperboloids or the parabolic quadric.

Although the surface procedure tested was a global technique, the influence of known points decreased as the distance away from these known points increased. Beyond this range of influence, the profiles became linear. As a result, the errors associated with these interpolated profiles were large. The area outside this range of influence could be considered as outside the convex shell of the data; in other words, the new values generated were extrapolations instead of interpolations.

Myers (1992) has added a function to the original interpolation equations to account for these extrapolation

errors. The exact form of this function has not yet been determined and is an area of on-going research.

There appeared to be a positive relationship between relative roughness and error. The closer the relative roughness was to 1, the larger the error. This appeared for the 5 largest average relative errors. With the Reynolds number, relative error showed the opposite relationship. The larger errors were at the smaller Reynolds number. This may indicate that the Reynolds number does not matter; relative roughness and not turbulence is the important variable.

From this study, it appears that to use multiquadrics with fluid speed, the number of sampled points need to be increased. Given the rapid change in fluid speed across a short vertical distance the number of points within a vertical needs to be increased, particularly in the region close to the bed.

The magnitude of the errors associated with the interpolation between the known points were, in some cases very large (e.g. over 100.00%), especially in the region close to the bed and in areas of rapidly changing flow. Given the magnitude of the errors associated with the interpolation and this application, it brings into question the error values associated with other interpolation techniques for fluid speed and other applications. Global circulation models of climate data, for example, are based on interpolations derived from a small number of scattered climate stations; this is

particularly true for areas of the southern hemisphere and the northern parts of North America. Perhaps there is a need to investigate further the magnitude of these errors for these techniques and different applications .

## **6.2 FUTURE RESEARCH**

This study, I believe, has opened up the avenue for a number of research areas in the field of multiquadrics and fluvial geomorphology. One of the areas that needs to be investigated is the role that distance plays in the value of interpolation. It appears that beyond a certain distance velocity profiles become completely linear. From the removal of odd numbered panels at CS11, this distance appears to be within 0.25 and 0.30 m of a known panel.

To test this idea, a data set with a greater sampling density is needed. In other words the distance between panels needs to be reduced. In the collection of fluid speeds, however, it is desirable to reduce the number of points sampled. Research is needed to find a way to maximize the results using interpolation routines given the number of control points. The optimum number of points needed to accurately describe the fluid speed surfaces with multiquadrics was not able to be determined from this study. The density of sampled points in different regions, rather than an absolute number, appears to be more important.

The role of stage also needs to be investigated. It is



possible that as the stage rises the magnitude of the errors may be reduced. An increase in stage would result in a decrease in relative roughness. As this parameter appears to be important in the size of the error, a potential reduction in error magnitude may result.

The error function of Myers (1992) also needs to be investigated. This study only examined one system - a gravel bed river with a relative roughness close to 1 and only one sampling procedure - speeds sampled at set locations at 10 verticals. It is possible that there maybe a family of values for this error function based on different channel geometries, depths, bed material and sampling procedure.

## REFERENCES

- Aho, A. K, B.W. Kernghan, and P. J. Weinberger. 1988. The Awk Programming Language. Reading, Mass. Addison-Wesley Pub. Co.
- Baker, V.R. and D.F. Ritter. 1975. Competence of rivers to transport coarse bedload material. **Geol. Soc. Amer. Bull.** 86: 975-978
- Best, J. L. 1988. Sediment transport and bed morphology at river confluences. **Sedimentology**. 35: 481-498.
- Boggs, S. Jr. 1987. Principles of Sedimentology and Stratigraphy. Merril Publishing Company, Toronto. 784 p.
- Bray, D.I. 1979. Estimating average velocity in gravel bed rivers. **American Soc. Civil Eng. J. Hydraulics Division**. 105(HY9): 1103-1122.
- Bridge, J. S. and S. L. Gabel. 1992. Flow and sediment dynamics in a low sinuosity, braided river: Calamus River, Nebraska Sandhills. **Sedimentology** 39: 1215-142.
- Bridge, J.S. and J. Jarvis. 1977. Velocity profiles and bed shear stress over various bed configurations in a river bend. **Earth Surf. Proc.** 2:281-294.
- Brooks, G.R. 1985. Current, erosional and depositional patterns at a river confluence and bend in the Nottawasaga River, Angus, Ontario. M.A Thesis, Wilfrid Laurier University, Waterloo, Ontario
- Carlson, R.E. and T.A. Foley. 1992. Interpolation of track data with radial basis methods. **Comp. Math. Applic.** 24(12): 27-34.
- Chapman, L. J and D.F. Putnam.1984. **The physiography of Southern Ontario**. Ontario Geological Survey, Special Volume 2, 270 pages.
- Chow, V. 1959. Open Channel Hydraulics. McGraw Hill Book Company Inc. New York. 680 pgs.
- Dietrich, W.E. and J. D. Gallinatti. 1991. Fluvial Geomorphology, In Field Experiments and Measurement Programs in Geomorphology. O. Slaymaker (ed). Univ. of British Columbia Press, Vancouver. 224 p.

- Environment Canada. Big Otter Creek Near Carlton Fact Sheet
- Fortier, S and F.C. Scobey. 1926. Permissible canal velocities. **Transactions A.S.C.E.** 89:940-984.
- Franke, R. 1982. Scattered data interpolation: tests of some methods. **Math. of Comp.** 38(157) : 181-200.
- Hadgigeorge, G. and J.E. Trotter. 1977. Short arc reductions of geos-3 altimetric data. **Geo. Res. Letters.** 4(6): 223-226.
- Hardy, R.L. 1971. Multiquadric equations of topography and other irregular surfaces. **J. Geophys. Res.** 76(8): 1905-1915.
- Hardy, R.L. 1972. Analytical topographic surfaces by spatial intersection. **Photogramm. Engng.** 38: 452-458.
- Hardy, R.L. 1977. Least squares prediction. **Photogramm. Engng.** 43: 475-492.
- Hardy, R.L. 1986. A multiquadric-biharmonic representation and approximation of disturbing potential. **Geo. Res. Letters.** 13(1): 18-21.
- Hardy, R.L. 1990. Theory and applications of the multiquadric-biharmonic method. 20 years of discovery 1968-1988. **Computers Math. Applic.** 19(8/9): 163-208.
- Hardy, R.L. and M. Gopfert. 1975. Least squares prediction of gravity anomalies, geoidal undulations, and deflections of the vertical with multiquadric harmonic functions. **Geo. Res. Letters.** 2(10): 423-426.
- Hassan, Y. A., T.K. Blanchat, C.H. Seeley Jr. and R.E. Canaan. 1992. Simultaneous velocity measurements of both components of a two-phase flow using particle image velocimetry. **Int. J. Multiphase Flow.** 18(3): 371-395.
- Hey, R. D. and C. R. Thorne. 1975. Secondary flows in river channels. **Area** 7: 191-195.
- Hickin, E.J. 1978. Mean flow structured in meanders of the Squamish River, British Columbia, **Can. J. Earth Sci.** 15(1): 1833-1849.

- Hjulstrom, F. 1935. Studies of the morphological activity of rivers as illustrated by the rivers Fyris. **Bull. Geol. Inst.** XXV.
- Jackson, R.G. 1975. Velocity-bed-form texture patterns of meander bends in the lower Wabash River of Illinois and Indiana. **Geol. Soc. Amer. Bull.** 86:1511-1522.
- Johnsonbaugh, R. and M. Kalin. 1989. Application Programming in C. McMillian Publishing Company. New York. 806 pgs.
- Komar, P.D. 1987. Selective gravel entrainment and the empirical evaluation of flow competence. **Sedimentology.** 34: 1165-1176.
- Lee, P.S., P.P. Lynn and E.M. Shaw. 1974. Comparison of multiquadric surfaces for the estimation of areal rainfall. **Hydrological Sciences Bull.** XIX 39: 303-317.
- Leighly, J. 1934. Turbulence and the transportation of rock debris by streams. **Geog. Rev.** 24:453-464.
- Leopold, L. and M.G. Wolman. 1960. River meanders. **Bull., Geol. Soc. Amer.** 71:769-794.
- Leopold, L., M.G. Wolman and J.P. Miller. 1964. Fluvial Processes in Geomorphology. W.H. Freeman and Co. 522 pgs.
- Martini, I. P. 1977. Gravelly flood deposits of Irvine Creek, Ontario, Canada. **Sedimentology.** 24: 603-622.
- Meland, N. and J. O. Norrman. 1966 Transport velocities of single particles in bed-load motion. **Geog. Ann.** 48A: 165-182.
- Menard, H.W. 1950. Sediment movement in relation to current velocity. **J. Sed. Petr.** 20(3): 148-160
- Middleton, G.V. and J.B. Southard. 1984. Mechanics of sediment transport. S.E.P.M short course number 3. 401 pgs.
- Morisawa, M. 1985. Rivers Forms and Processes. Longman Group Limited. 222 p.
- Myers, D. E. 1992. Kriging, Cokriging, radial basis functions and the role of positive definiteness. **Computers Math. Applic.** 24(12): 139-148.

- Nordin, C. F. Jr. 1963. A preliminary study of sediment transport parameters, Rio Puerco near Bernado, New Mexico. **US Geol. Survey, Prof. Pap.** , 462 F, 35 p.
- Plauger, P.J.. 1992. The Standard C Library. New Jersey. 498 p.
- Press, W. H., B.P. Flannery, S.A Teukolsky and W. Vetterling. 1988. Numerical Recipes in C: the Art of Scientific Computing. Cambridge University Press, 735 p.
- Robert, A., A. G. Roy and B.DeSerres. 1992. Changes in velocity profiles at roughness transitions in coarse grained channels. **Sedimentology** 39: 725-735.
- Saunderson, H.C. 1992. Multiquadric interpolation of fluid speeds in a natural river channel. **Comp. Math. Applic.** 24(12): 187-193.
- Saunderson, H.C. (1994a). Multiquadric surfaces in C. **Comp. & Geoscienc.** 20(7/8): 1103-1122.
- Saunderson, H.C (1994b). Multiquadric of scalar and vectorial quantities in physical geography. Presentation to the Canadian Association of Geographers. May, 1994. Waterloo, Ont.
- Saunderson, H.C and G.R. Brooks. (in press). Multiquadric sections from a fluid vector field: in Kansa, E.J. (ed.), Special issue on theory and application of radial basis functions. **Int. Journ. Sci. Computing and Modeling.**
- Saunderson, H.C. and F.P.J. Lockett. 1983. Flume experiments on bedforms and structures at the dune-plane bed transition, In Moderns and Ancient Fluvial Systems. J.D. Collinson and J. Lewin, editors. 6: 49-58, Internat. Assoc. Sedimentol., Spec. Pub.
- Savini, J and G.L Bodhaine. 1971. Analysis of current-meter data at Columbia River Gauging Stations, Washington and Oregon. **US Geol. Survey Water Supply Paper**, 1869-F: 43 pp.
- Schiro, R. and G. Williams. 1984. An adaptive application of multiquadric interpolants for numerically modelling large numbers of irregularly spaced hydrographic data. **Surveying and Mapping.** 44(4): 365-381.
- Shaw, E. M and P.P. Lynn. 1972. Areal rainfall evaluation using two surface fitting techniques. **Bull. Int.**

**Ass. Hydrol. Sci.** 17(4): 419-433.

Sibul, U. 1969. Water resources of the Big Otter Creek drainage basin. Water Resources Report 1. Ontario Water Resources Commission. Toronto. 91 pgs.

Sirayanone, S. 1988. Comparative studies of kriging, multiquadric-biharmonic, and other methods for solving mineral resource problems. Unpub. Ph.D. Dissertation, Iowa State Univ., Ames, Iowa, 355 p.

Sundborg, 1967. Some aspects on fluvial sediments and fluvial morphology. I General views and graphic methods. **Geogr. Annaler.** 49: 333-343.

Tabios III., G.Q. and J.D. Salas. 1985. A comparative analysis of techniques for spatial interpolation of precipitation. **Wat. Res. Bull.** 21(3): 365-380.

Vanoni, V.A. 1966. Sediment transportation mechanics: initiation of motion. **Journ. Hydraulics Division, A.S.C.E.** HY2:291-314

Water Survey of Canada. 1986. Suspended Sediment Collection Manual. Ottawa. 197 pages.

Watson, D.F. Personal Communication, 1994.

Watson, D. F. 1992. Contouring: a guide to the analysis and display of spatial data. Pergamon Press. 321 pgs.